HIGH RESOLUTION GEOCHEMISTRY OF THE CRETACEOUS EAGLE FORD FORMATION, BEE COUNTY, TEXAS

by

LISA MICHELLE MORAN

Presented to the Faculty of the Graduate School of

The University of Texas at Arlington in Partial Fulfillment

of the Requirements

for the Degree of

MASTER OF SCIENCE IN GEOLOGY

THE UNIVERSITY OF TEXAS AT ARLINGTON

December 2012

ACKNOWLEDGEMENTS

First of all, I would like to thank Dr. Harry Rowe for all of his wisdom, guidance and support during this process. Without a guide to navigate graduate school, I could have easily been lost.

I would also like to thank Dr. John Wickham and Dr. Andrew Hunt for their mentorship as members of my graduate committee. Their support and advice helped to make this project possible. Additionally, I would like to thank Dr. Stephen Ruppel of the Bureau of Economic Geology for providing access and academic support for this project.

To the members of the Fort Worth Geological Society, financial support of this project was greatly appreciated.

Throughout my academic journey, Dr. Merlynd Nestell and Dr. Galina Nestell have provided support, both personal and academic, that has allowed me to strive for excellence, accept challenges and believe that all things are possible. I will be eternally grateful.

Thanks also to Dr. William Smith. He is one of the first professors to show me that being a returning student did not diminish my capabilities in any way. He also taught me one of my most valuable life lessons for when I fail, I will always "fail with gusto."

Without a solid personal support system, academic achievement, especially as a non-traditional student, is almost impossible. I would like to extend my thanks to my friends and colleagues: Angie Osen, Amber Cunti, Krystin Robinson and James Hoelke. My gratefulness for the years of phone calls, emails, text messages, pity pansies and constant encouragement cannot be overstated.

Lastly, I would like to thank the members of my family. I absolutely could not have done this without your constant love and support. As a wife and a mother, academic endeavors constantly conflict with family time and obligations. More often than not, school had to be

prioritized over family time. For my son, Josh, and my husband, Mike, their sacrifice of family time and unconditional support helped make my academic success possible.

My extended family, especially Sue Petzold and Ray McClendon, have also provided very much appreciated and unconditional support for my academic career.

And for my parents, Chuck and Mary Pridgeon, they taught me that "no" usually means there is another way around a problem and to do whatever it takes to make things happen the way I want them to. Their unwavering belief in me and what I could accomplish helped keep my head above water, especially when I had my own doubts.

Thank you all so very much.

November 26, 2012

ABSTRACT

HIGH RESOLUTION GEOCHEMISTRY OF THE CRETACEOUS EAGLE FORD FORMATION, BEE COUNTY, TEXAS

Lisa Moran, M.S.

The University of Texas at Arlington, 2012

Supervising Professor: Harry Rowe

The Eagle Ford Formation of Bee County, Texas is a sporadically laminated carbonaceous dark mudrock. The depositional area of the Eagle Ford Formation stretches across the state of Texas in a northeast-southwest trend. Early studies of the Eagle Ford found the deposits to be rich in organic material but could not fully describe the formation due to the lack of outcrop exposure. Recent studies of the Eagle Ford Formation have begun to explore the sub-surface nature of the formation.

Geochemical analyses of the J.A. Leppard #1 core from the southwestern portion of the formation was conducted to further constrain the sub-surface geochemical signatures of the Eagle Ford Formation. Major and trace element compositions were all measured using a hand-held X-ray fluorescence spectrometer. Bulk geochemistry, trace metal enrichments, inferred mineralogy and geochemical relationships were used as proxies to define the depositional paleoenvironment and degree of basin restriction.

The Eagle Ford Formation was deposited under mostly anoxic/euxinic conditions with intermittent pulses of oxygenation. The basin was mostly restricted, but with significant periods of a more open marine setting. Dark mudstones associated with similar depositional histories have previously been linked to global Cretaceous oceanic anoxic events (OAEs).

Earlier studies inferred that the Eagle Ford Formation preserved in the J.A. Leppard #1 core preserved a record of the Cenomanian-Turonian boundary. However, biostratigraphic evidence questions the original timing of sedimentation at the core location. It is now believed that the chemostratigraphic patterns could be related to marine preconditioning episodes of anoxia/euxinia prior to a major OAE.

TABLE OF CONTENTS

LIST OF ILLUSTRATIONS

LIST OF TABLES

CHAPTER 1

INTRODUCTION

1.1 Geochemical Analysis

Chemostratigraphic analyses of drill core samples can yield insight into the possible paleo-conditions of the water column, organic matter burial information, diagenetic history of a formation and global-scale changes in paleoclimate conditions.

Major and trace element quantification of rock cores has been used to interpret paleo-conditions such as primary productivity, degree of basinal restriction, deepwater renewal times, the presence or absence of hydrogen sulfide, redox conditions and for estimating the prior levels of oxygen in the water column (e.g.Calvert, 1987; Dean and Arthur, 1989; Piper, 1994; Algeo and Maynard, 2004; Piper and Perkins, 2004; Rimmer, 2004; Algeo et al., 2008; Rowe et al., 2008; Piper and Calvert 2009; Algeo and Rowe, 2011). By comparing the enrichment factors (EFs) of specific trace metals against "average gray shale" (Wedephohl, 1971). The chemical signatures of water column conditions can also be inferred (Calvert and Pederson, 1993; Crusius et al., 1996). Vanadium (V), nickel (Ni), molybdenum (Mo), copper (Cu) and uranium (U) have been successful proxies in approximating paleo-conditions of marine waters (Jones and Manning, 1994; Hastings, 1996; Algeo and Maynard, 2004; Algeo and Lyons, 2006; Brumsack, 2006; Algeo and Tribovillard, 2010).

Major element cross plots can give an indication of the down-core (stratigraphic) changes in mineral content. For instance, if there is a positive covariance in the cross plot of iron (Fe) and sulfur (S), the mineral most likely involved is pyrite (FeS_2). If no covariance occurs, the elements are unlikely to be present in the same mineral phase.

Positive and negative excursions of stable isotope ratios of organic carbon ($\delta^{13}C$), nitrogen ($\delta^{15}N$) and oxygen ($\delta^{18}O$) found in the organic matter component of marine shales have been utilized in similarly unraveling the paleo-oceanographic conditions. By comparison to modern analogues, the ratios can be useful in approximating the sources of organic matter, correlating large-scale carbon accumulations due to possible global anoxic marine conditions and rates of paleoproductivity (Meyers, 1988; Meyers, 1994; Twichell et al., 2002).

This study addresses the geochemical signature of the Eagle Ford Formation in Bee County, Texas. By utilizing the above mentioned strategies, assessment of the Cretaceous rock unit will further constrain the prerequisite paleo-conditions of the area.

1.2 Geological Information

1.2.1 History

The Eagle Ford Formation has been designated with varying stratigraphic nomenclature from the East Texas Basin to the West Texas Maverick Basin. R.T. Hill originally described the type locality and named the formation after the town of Eagle Ford, near Dallas, Texas (Hill, 1901). The Eagle Ford Formation in outcrop is "mostly blue and black laminated shale, which grades upwards into a brown weathered section of ferruginous glauconitic sand interlaminated with clay" (Gordon, 1911; Surles, 1987). The Eagle Ford Formation of north-central Texas was later divided into the Tarrant, Britton and Arcadia Park Formations. (Sellards et al., 1932). The Tarrant Formation "consists of 15 to 20 feet of grey to brownish-grey calcareous sandstone interbedded with brown siltstone, brownish limestone and shale (Brown and Pierce, 1962). The Britton and Arcadia Park Formations both consist of "laminar calcareous mudstone interbedded with thin impure beds of limestone and siltstone" (Brown and Pierce, 1962; Surles, 1987). Surles further described the Eagle Ford Group of the East Texas Basin to include the Sub-Clarksville Sand Formations: the lower Bells Sandstone member and the upper Maribel Shale member (McNulty, 1966; Surles 1987). The Eagle Ford in West Texas includes the equivalent

Boquillas Formation and is divided into the Langtry and Rock Pens members (Surles, 1987; Lock and Peschier, 2006; Donovan and Staerker, 2010). The "flaggy limestones, with high organic and terrigenous content and low faunal diversity that occurred between the Buda Limestone and Austin Chalk" were originally named the Boquillas Flags Formation (Udden, 1907; Donovan and Staerker, 2010). Beginning in the 1950's, geoscientists began to refer to the Boquillas as the Eagle Ford. Even though the nomenclature is inconsistent in naming the Eagle Ford across Texas, bounding parameters of the Eagle Ford remain generally the same. In most instances, the Eagle Ford rocks are considered to unconformably lie under the Austin Chalk and unconformably cap the Buda Limestone (Pessagno, 1969; Surles, 1987; Hentz and Ruppel, 2010; Harbor, 2011) (Figure 1.1).

The upper Cretaceous deposits in the Texas portion of the Gulf Coast were biostratigraphically correlated to the geologic time scale by fossil foraminifera, nannofossils and ammonites (Sohl and Smith, 1980; Mancini et al., 1996, Mancini and Puckett, 2005; Scott, 2010). Jiang assigned the Eagle Ford Shale to the Cenomanian-Turonian stages based upon ammonite distribution and Foraminifera assemblages (Jiang, 1989). Radiometric dating positioned the Cenomanian-Turonian boundary (~92 Mya) in the uppermost portion of the Eagle Ford Formation (Dawson, 2000; Keller and Pardo, 2005).

The Eagle Ford Formation has been extensively examined in outcrop in East and Central Texas (Hill, 1901; Gordon, 1911; Sellards et al, 1932; Brown and Pierce, 1962; McNulty, 1966; Surles, 1987; Dawson, 2000). The West Texas equivalent, known as the Boquillas Formation, has also been studied in outcrop and in the subsurface (Lock and Peschier, 2006; Lock et al.,

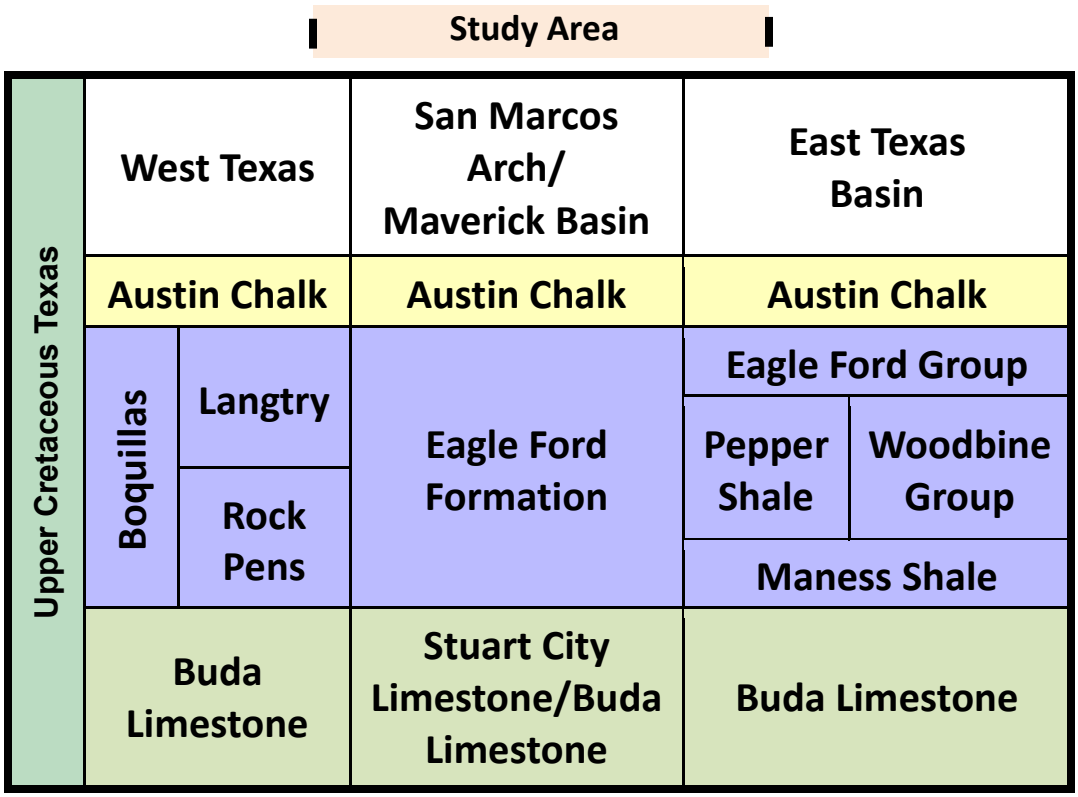

Figure 1.1 Stratigraphic column of the Eagle Ford Formation. Modified after Phelps, 2011.

2007; Donovan and Staerker, 2010). The Eagle Ford play has not been fully defined in the literature, in part, because a large portion of the succession is located in the subsurface and regional and correlative studies of well logs and subsurface characteristics have only recently been published (Hentz and Ruppel; 2010; Harbor, 2011; Phelps, 2011).

The rocks in the greater study area (Texas) have been referred by several different names: the Eagle Ford Group, Eagle Ford Shale and Eagleford. However, for the sake of clarity, nomenclature used by Hentz and Ruppel (2010) will be utilized and the study area will be referred to as the Eagle Ford Formation. It must also be noted that the fissillity of "shale" as defined by Underwood "an argillaceous rock possessing lamination or fissility" is not strictly

characteristic of the nature of the Eagle Ford Formation deposits (Underwood, 1967). While laminations are present, a degree of fissility is distinctly absent. A more correct Underwood classification would be the term "mudrock." The terms mudrock and shale are incorrectly used interchangeably in the literature (Kuypers, 2001; Kolonic et al., 2005; Hetzel, 2008). For the purpose of this study, the term mudrock will be utilized.

1.2.2 Paleogeographic Setting

During the Cretaceous, from the late Albian stage to the end of the Maastrichtian, a significant portion of the North American craton was covered by marine waters (Figure 3). Periodically, these marine waters, also known as the Western Interior Seaway (WIS), stretched from Arctic Canada, in the North, to the Gulf of Mexico, in the South, at the maximum flooding extent (Kauffman, 1984)(Figure 1.2). The WIS was flanked to the east by the stable North American craton and in the west by a Cordilleran thrust belt with "volcanic centers localized in Idaho-Montana and New Mexico-Arizona" (Kauffman, 1977). The southern edge of the North American shoreline, from Florida through Texas and Mexico, also referred as the "proto-Gulf of Mexico," contained a broad, stable shelf complex, subjected to repeated deposition and erosion (Murray et al., 1985; Scott, 2010). The WIS recorded five major transgressive-regressive cycles throughout its history (Kauffman, 1984)

The Cretaceous section of Texas is divided into three long-term depositional cycles: the Coahuila Series, the Comanchean Series and the Gulfian Series (Surles, 1987). At least seven different cycles of shallow water carbonates overlain by fine-grained clastics have been recorded within the three series. The strata are separated by unconformities interpreted to represent transgressive-regressive depositional episodes. The Coahuilan Series is the oldest, starting from the base of the Berriasian, and continues until the inter-Aptian unconformity.

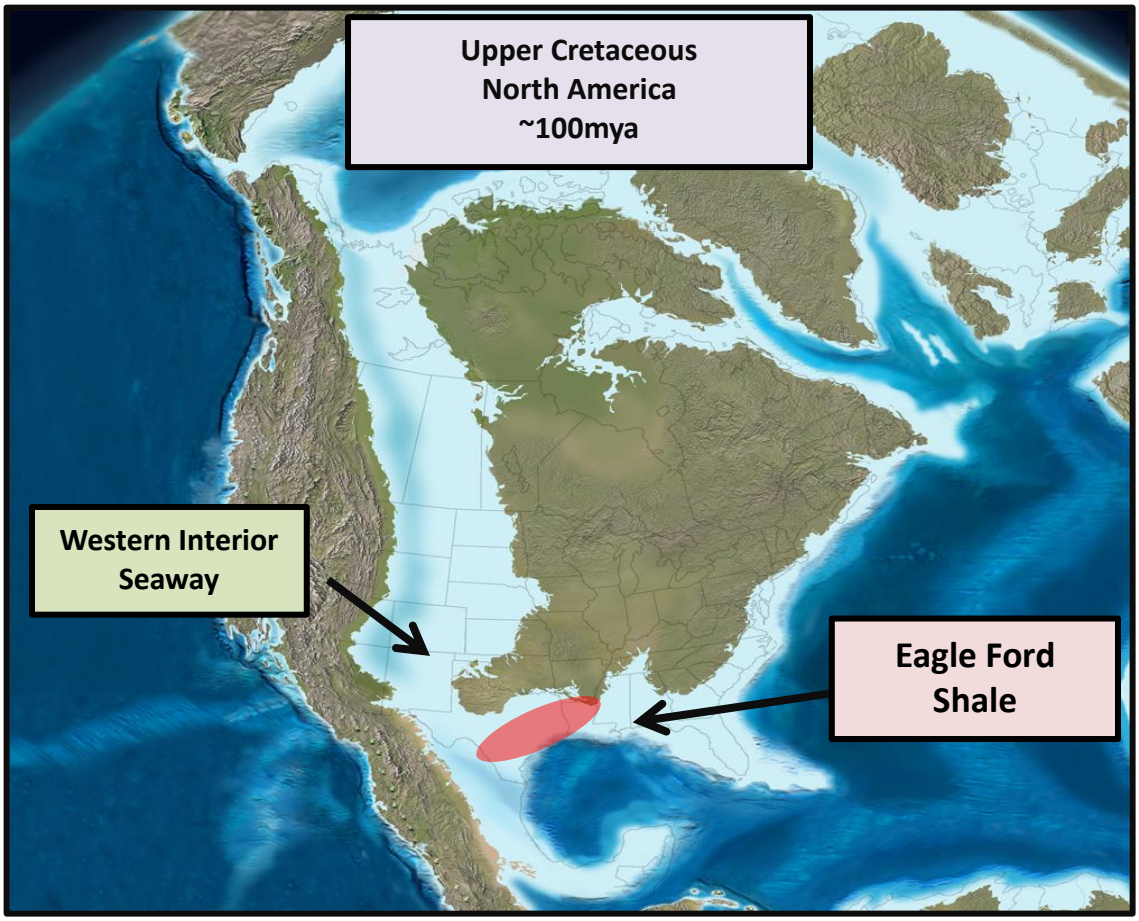

Figure 1.2 Western Interior Seaway of Cretaceous North America. Modified after Blakey, 2012. Eagle Ford depositional area highlighted in red.

The next series, the Comanchean, extends through to the intra-Cenomanian boundary. Everything above the Buda Limestone, including the Eagle Ford Formation, is considered to be part of the Gulfian Series. The Eagle Ford Formation is believed to represent deposition on inner to outer marine shelves during one of these events (Surles, 1987; Scott, 2010).

1.2.3 Characteristics

From the southwestern-most Eagle Ford (Boquillas) succession in the Maverick Basin, the Eagle Ford extends 250 miles in the north east direction into the East Texas Basin. Depths of

the deposits in the Maverick Basin have been measured to at least 15,600 feet. Across the top of the San Marcos Arch, Eagle Ford deposits thin to less than 100 feet. The East Texas Basin includes the Eagle Ford Formation and the lithologically divided; Maness and Pepper Shales. Woodbine fluvial deposits assigned to the Cenomanian are also found in the East Texas Basin, although their exact relationship to the Eagle Ford Formation has yet to be determined (Hentz and Ruppel, 2010).

Overall, in the southern portion of the area, Eagle Ford facies represent two different depositional units. The lower interval is considered to represent transgressive conditions and includes pyritic and fossiliferous shales, along with bituminous claystone and shales. The upper interval is considered to be a regressive sequence which includes fossiliferous shales and silty (quartzose) shales (Dawson, 2000). In the San Marcos Arch area, the total unit characteristically has a high total organic content (TOC) of ~1 to 8 wt.% with an average of 3.9% and the lower unit having higher values than the upper unit (Dawson et al, 1993; Liro et al, 1994). The lower unit shows a high gamma ray value of 20-135 API (American Petroleum Institute) units on well logs. It is a mostly dark grey mudrock with some calcareous mudrocks, marls and limestone. The upper unit usually shows lower API values, from 45-60 API units. On well logs, both units can be identified by their gradational contacts with the units above them. The upper unit, in particular, shows a distinct gradational contact with the Austin Chalk (Hentz and Ruppel, 2011). Across the San Marcos Arch, the lower unit is mostly represented with only a thin strip of the upper unit found along the crest of the arch. In the East Texas Basin, the calcareous upper unit is missing but the lower, organic-rich unit, is present (Hentz and Ruppel, 2010) (Figure 1.3).

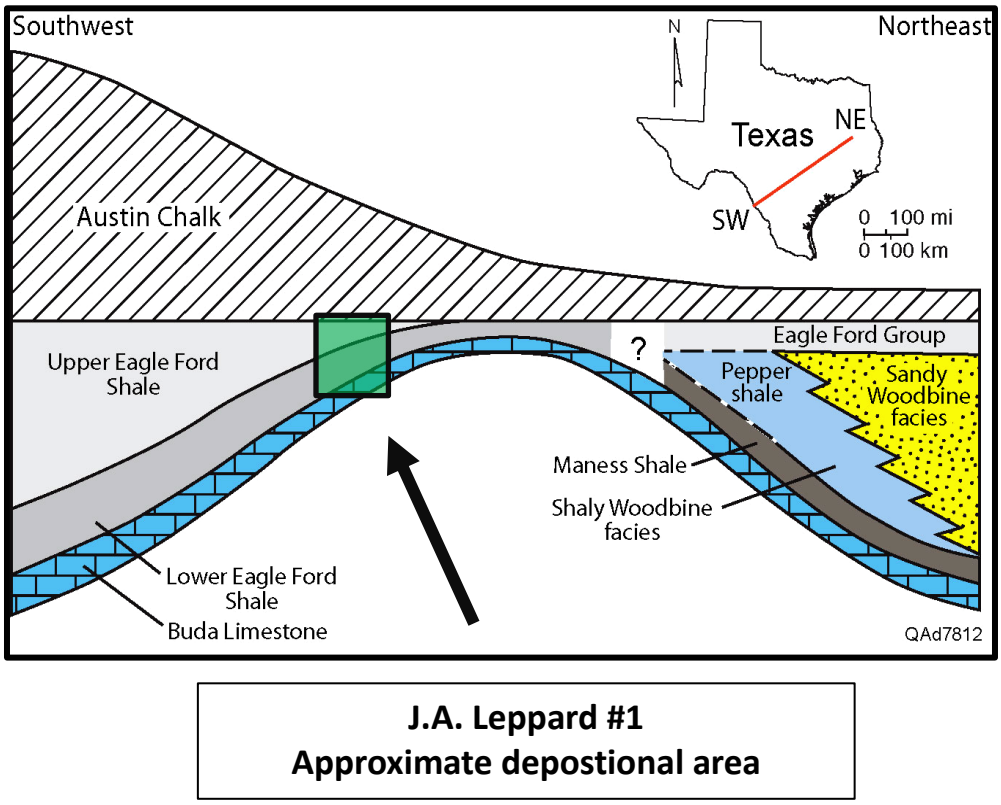

Figure 1.3 Northeast-southwest cross section of Eagle Ford distribution. (Hentz and Ruppel, 2010).

1.2.4 Paleoclimate

The occurrence of Cretaceous-age organic rich mudrocks in the WIS basin has been shown to correlate with the globally correlated Oceanic Anoxic Events (OAEs) and global sea-level changes (Gale et al, 2008). Thick black shales with little bioturbation and characteristic fine laminations have been liked to global perturbations in marine water chemistry, increased atmospheric CO_2, increased volcanic activity, sluggish circulation and large-scale marine transgressions (Schlanger and Jenkyns, 1976; Jenkyns, 1980; Arthur et al, 1988; Arthur and Sageman, 1994; Algeo et al., 2008). The decreased oxygen content of Cretaceous marine waters at the time of the OAEs provided some of the mechanisms for massive deposits of

organic material to be preserved. OAEs consistently record significant positive excursions of $\delta^{13}C$ of organic carbon due to the increase of buried organic carbon material (Arthur and Schlanger, 1979; Arthur et al., 1988).

The causal factors of the OAEs around the world are currently under debate. Strontium isotope excursions have been related to seafloor hydrothermal activity (Jones and Jenkyns, 2001). Increased phosphorous and subsequent biological oscillations have also been cited as factors in widespread ocean anoxia (Handoh and Lenton, 2003). Rapid sea level changes possibly contributed to the fluctuating levels of oxygen in the ocean by disturbing the circulation patterns and creating a more stratified water column (Leckie et al., 2002).

One of these global events, termed OAE2 is documented at the Cenomanian-Turonian boundary (Arthur et al., 1979). Other significant Cretaceous OAEs include the T-OAE during the early Toarcian, OAE 1a during the early Albian, and a mid-Cenomanian event termed MCE (Jenkyns, 2010; Coccioni and Galeotti, 2003). Previously published studies suggest the Eagle Ford Formation preserves Cenomanian-Turonian boundary, thus, OAE2 is also recorded in the deposits (Berner and Raiswell, 1983; Comet, 1993; Dawson, 1997; Kearns, 2011).

1.3 Economic Importance

The Eagle Ford Formation is part of the northeast-southwest trending Upper Cretaceous Gulfian Series in Texas currently being explored for natural gas and oil. There are approximately 5000 permits filed with the Texas Railroad Commission for drilling in the Eagle Ford Formation Play with almost 3000 wells completed and on schedule. As of August 2012, the Eagle Ford Formation Play is producing 297,079 barrels of oil and 880 MMcf of natural gas per day (Railroad Commission of Texas, 2012). The oil and dry gas windows of this play suggest the hydrocarbons thermally mature in a southerly direction denoting the variability of conditions within the play (Figure 1.4). Fully understanding the extent of and variability within the play becomes increasingly economically and academically important.

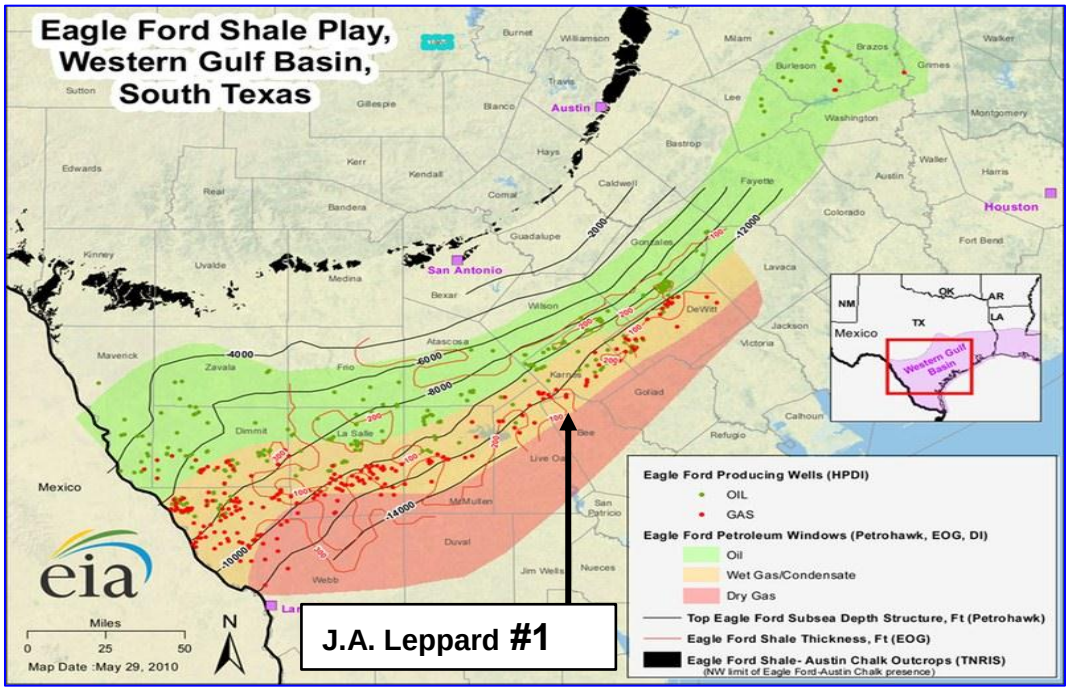

Figure 1.4 Eagle Ford Formation Play. Western Gulf Basin, South Texas. (Railroad Commission, 2012)

CHAPTER 2

METHODS

2.1 Drill Core Information

The J.A. Leppard #1 (API 4202530389) drill core is currently located in the core repository of the Texas Bureau of Economic Geology (BEG) at the Pickle Research Center in Austin, Texas. Boxes 1-19 of 49 total core boxes were studied at a depth interval of 13531-13671 feet. A total of 830 samples were analyzed. The diameter of the J.A. Leppard #1 core is 4 inches. Drilling of the J.A. Leppard #1 started on July 15, 1975 in the northwest portion of Bee County, Texas. Facies characterizations and stratigraphy were identified by University of Texas at Austin graduate student, Ryan Phelps, in his 2011 PhD dissertation manuscript.

2.2 Energy Dispersive X-Ray Fluorescence (ED-XRF)

Core samples were marked using chalk prior to ED-XRF analysis at an approximately three-inch interval. A Bruker Tracer III-V handheld ED-XRF (BEG-1) spectrometer was used to measure metal concentrations in each sample. The instrument was stabilized using a plastic platform supplied by Bruker. Samples were placed on the nose of the instrument immediately above the 3x4 mm elliptical beam window and stabilized using a platform that surrounded the instrument's nose. Because the measurement sensitivity of the ED-XRF instrument decreases by the inverse square of the distance from the silicon detector (SiPIN), located directly beneath the sampling window, a flat sample surface is needed in order to optimize measurement consistency and accuracy. Core samples were analyzed on the clean and dried, slabbed side

whenever possible. Samples that were not suitably flat were mechanically stabilized or given a flat surface area for analysis.

Two phases of data acquisition were undertaken on each marked stratum. The inorganic elemental suite was generated using two separate and distinct data acquisitions for each sample. Major element data acquisition, including V and Cr measurements, was undertaken using a low-energy, vacuum-pumped instrument setting; trace element data acquisition was undertaken using a filtered, high-energy instrument setting. Both low and high energy analyses were undertaken at the same location on the core face, marked by yellow chalk. Major lithoclasts were avoided to minimize unrepresentative measurements.

Low-energy spectrum acquisition includes elements that emit characteristic x-rays between 1.25 to 7.06 kV. In order to obtain the elements in this range, and allow for backscatter that does not interfere with the peaks of interest, the voltage on the instrument was set to 15 kV. The instrument current was set to 42 μA; however, while the voltage settings remain constant for this elemental range, regardless of the Tracer III-V used, the current settings vary between instruments due to the inter-instrument variability associated with the manufacture of the x-ray tube and electronics. In addition, instrument sensitivity to lighter elements (below and including Ca) was increased through the use of a vacuum pump, which removes the air between the sampling window and the detector. A vacuum pump operating at <3 torr was attached directly to the Tracer III-V.

The characteristic x-rays between 6.92 and 19.80 kV were measured in the high-energy acquisition mode (40 kV and 28 μA). While a filter was used to prevent the low-energy x-rays from reaching the detector, a vacuum pump was not necessary because the energies of x-rays emitted from heavier elements are not attenuated in the short distance between the sample and the detector. The filter consists of 0.006” Cu, 0.001” Ti, and 0.012” Al and is inserted directly into the instrument. High-energy acquisitions were taken for 3 minutes. Low-energy acquisitions were taken for 1 minute.

2.2.1 ED-XRF Mudrock Calibration

The raw spectra obtained during the Tracer III-V acquisition are qualitative and require a calibration to convert the data into quantitative weight percentages. The calibration for the handheld ED-XRF unit is matrix-specific, so a calibration for major and trace elements of mudrocks was developed using a suite of 90 reference materials (Rowe et al., 2012). The calibration includes the following 90 mudrock standards: 5 international, 7 Devonian-Mississippian Ohio Shale, 20 Pennsylvanian Smithwick Formation of Central Texas, 27 Devonian-Mississippian Woodford Formation of West Texas, 15 Late Cretaceous Eagle Ford Formation of South Texas, and 16 Mississippian Barnett Formation of North-Central Texas.

Each of the 90 reference materials were pulverized in a TM Engineering Pulverizer with trace-metal grade grinding barrels to 200 mesh. Approximately 8 grams of each of the powdered standards with a boric acid backing were pressed using a Carver press to 40 tons with a 40 mm die. The finished reference pellets were analyzed for major and trace elements using wavelength-dispersive x-ray fluorescence (WD-XRF) and inductively-coupled plasma mass spectrometry (ICP-MS), respectively.

The standard pellets were analyzed on the Bruker Tracer III-V for six minutes at three different locations on the pellet face under both low and high energy settings. All 270 raw x-ray spectra (90 references x 3 analyses) were loaded into Bruker's CalProcess software along with the accepted (WD-XRF & ICP-MS) elemental concentrations for all standards. Low energy and high energy calibrations were developed by making inter-element corrections (slope and background) for each element in each calibration. Certain standards were omitted after the implementation of the inter-element corrections using statistical analysis for each element to determine the outliers with a standardized value greater than 3.0 standard deviations from the mean.

The completed calibration yields quantified values using the raw ED-XRF spectra from unknown samples. The low energy calibration quantifies the following elements: Mg, Al, Si, P,

S, K, Ca, Ba, Ti, V, Cr, Mn, and Fe. The high energy calibration quantifies the following elements: Ni, Cu, Zn, Th, Rb, U, Sr, Y, Zr, Nb, and Mo. The limits of determination of a method (LDM) for each element (Table 2.1) are provided (Rowe et al., 2012).

2.3 Non-XRF Geochemical Data

The measurements for total organic carbon (TOC), total nitrogen, and the stable carbon and nitrogen isotopes ($\delta^{13}C$ and $\delta^{15}N$) of TOC and total nitrogen (TN), respectively, were compiled by T.J. Kearns for his MS thesis work in 2011. The methods used by Harry Rowe and described by Kearns, pertinent to this study, are included for clarity for the comparisons and utilization of data in this study. For certain ratios and comparisons, data at specific depths were normalized from this study to Kearns' depths. The present study scanned the core at a 3 inch resolution and Kearn's study scanned the core at a 1 foot resolution.

2.3.1 TOC-TN-δ13C-δ15N

"Total organic carbon (TOC), total nitrogen (TN), and stable isotopic compositions of TOC ($\delta^{13}C_{TOC}$) and ($\delta^{15}N_{TN}$) were performed on powdered samples that were weighed into silver capsules (Costech Analytical, Inc. #41067) and subsequently acidified repeatedly with 6% sulfurous acid (H_2SO_3) in order to remove carbonate phases (Verardo et al., 1990). Samples were analyzed at the University of Texas at Arlington using a Costech ECS 4010 elemental analyzer interfaced with a Thermo Finnigan Conflo IV device to a Thermo Finnigan Delta-V isotope-ratio mass spectrometer (IRMS). Isotopic results are reported in per mil (‰) relative to V-PDB for $\delta^{13}C$ and air for $\delta^{15}N$. The average standard deviations were 0.13‰ and 0.08‰ for $\delta^{13}C$ and $\delta^{15}N$ of USGS-40 glutamic acid (IAEA-8573), respectively, and 0.39% and 0.01% for the TOC and TN of USGS-40, respectively. The average standard deviations for unknown samples analyzed in triplicate were <0.2‰ for both $\delta^{13}C$TOC and $\delta^{15}N_{TN}$, and 0.1% for both TOC and TN" (Kearns, 2011).

2.3.2 X-Ray Diffraction (XRD)

For methods used in x-ray diffraction please refer to Jack Kearns' thesis (Kearns, 2011).

2.3.3 General XRF and Non-XRF units

The graphs, cross plots and ternary diagrams in the following sections have units in weight percent (e.g. %Si), parts per million (e.g., ppm Sr), degree of pyritization (DOP_T), per mil (‰), whole number ratio (C/N), or are expressed in enrichment factors (EFs).

$$DOP_T = \text{pyritic iron/total iron (Raiswell and Berner, 1986)}$$

$$EF = (\text{element in ppm/Al in ppm})_{sample} / (\text{element in ppm/Al in ppm})_{standard}$$

Ternary plots use normalized data. Some cross plots will also utilize major and trace metal content normalized to aluminum (Al) in order to mitigate the clay fraction of the sample. The J.A. Leppard #1 data points were divided into the following color scheme to distinguish between the chemostratigraphic depths of the Austin Chalk (AC) and four subdivided zones of the Eagle Ford Formation: A,B,C and D. The divisions were based upon the amplitudes of the oscillations in trace metal enrichment factors and major elemental content. Zone A does not contain a high degree of oscillations and has only one major excursion. Zone B contains the majority of the high amplitude oscillations. Zone C indicates few oscillations and an excursion. Zone D has in increase in oscillations and an increase in amplitude. Zone C indicates little trace metal enrichment but some distinct oscillations in major metal content (Figures 2.1 and 2.2).

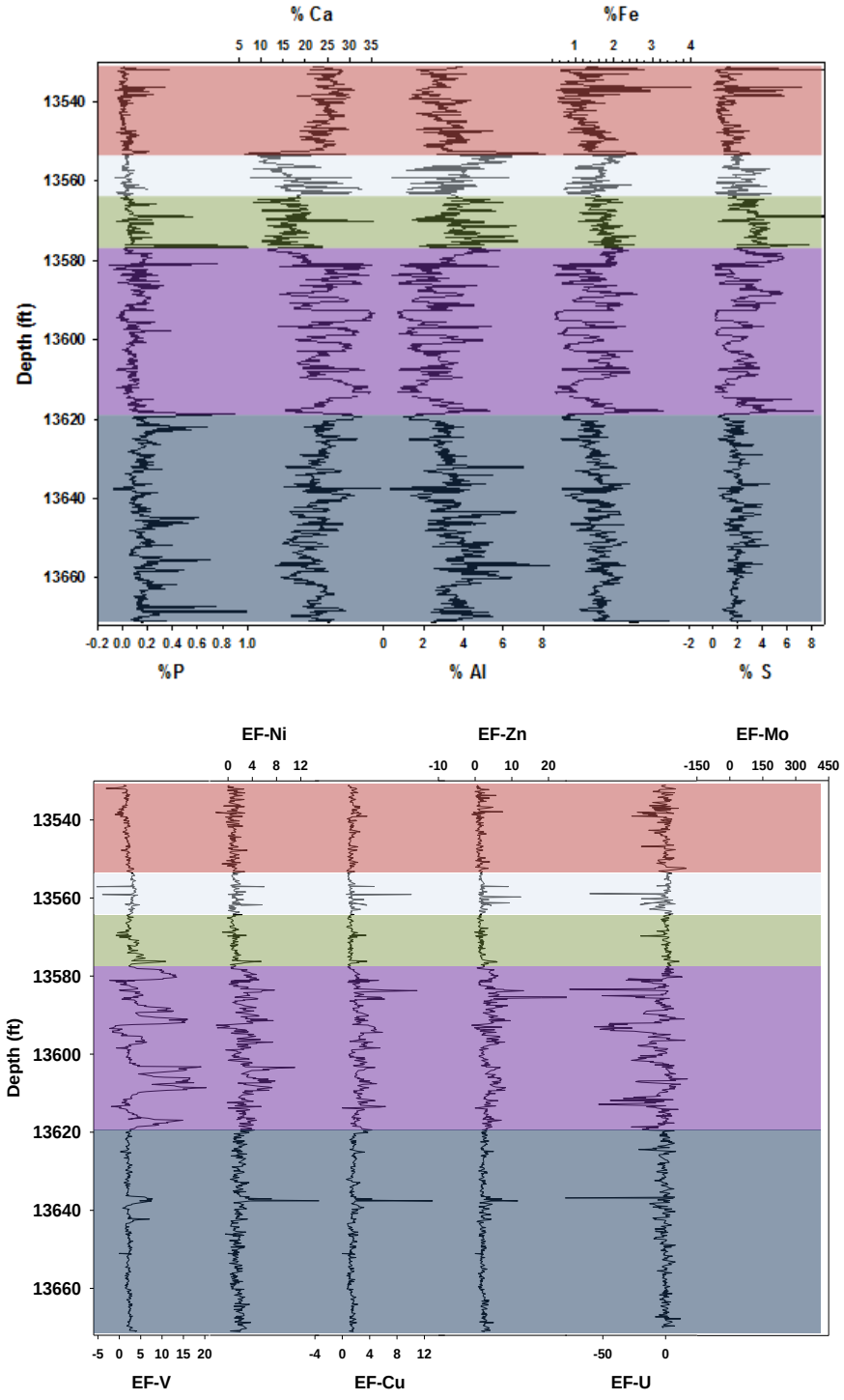

Figure 2.1 Zone differentiation

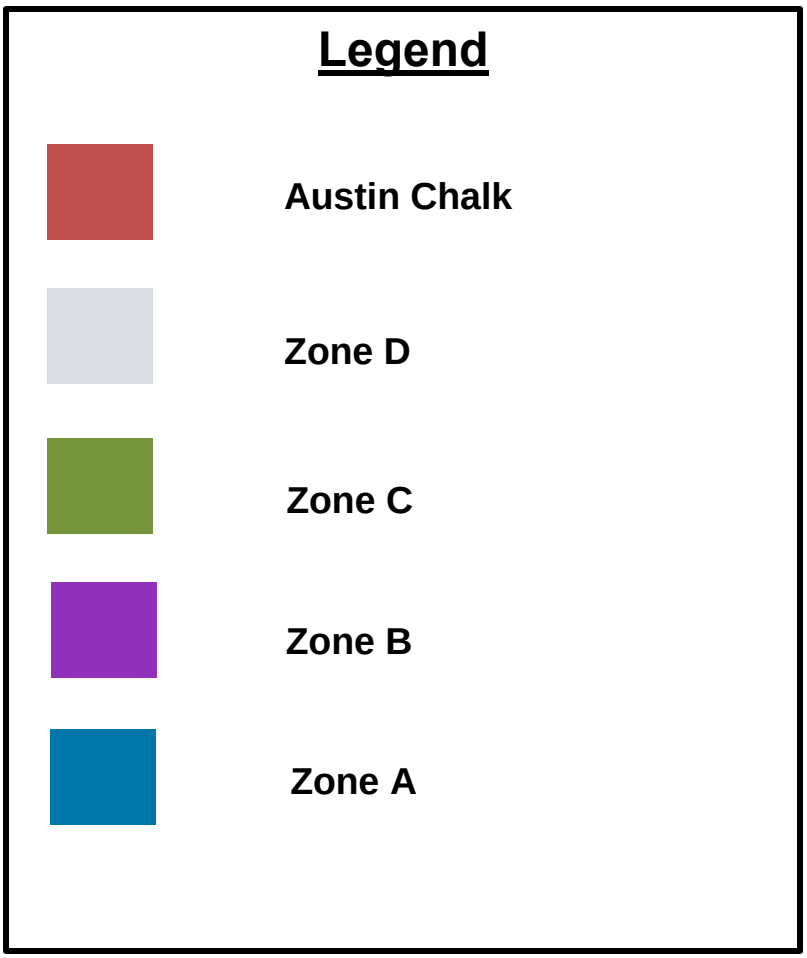

Figure 2.2 Color scheme for diagrams.

CHAPTER 3

RESULTS

3.1 Physical Description

Approximately 142 feet of the J.A. Leppard #1 core were examined in the present study. The Austin Chalk (13531-13552 ft.) and the Eagle Ford Formation (13552-13671 ft.) represented in this core. The Eagle Ford Formation was lithologically divided around 13552 ft. into upper and lower Eagle Ford sections. The Stuart City Limestone was not scanned for this study. The upper most Austin Chalk member was a light grey, slightly laminated calcareous mudstone with limited pyrite inclusions, *Zoophycos* burrows and discrete ash layers. The upper portion of the Eagle Ford Formation, immediately beneath the Austin Chalk contact, was a dark grey, slightly laminated calcareous mudstone with several layers of ash. The upper Eagle Ford section was highly fissile in the vicinity of the ash layers with visible sulfur-rich coatings. The lower Eagle Ford section was a medium to dark grey argillaceous mudstone with an increase in lighter, calcareous, laminations compared to the upper section. Select portions of the lower Eagle Ford had a marly appearance. Some of the laminated portions had visible abrupt changes in coloration and magnitude of laminations. Ash layers were also present. Lamination frequency increased with depth. Infrequent *Inoceramus* fragments were found in both the upper and lower portion of the Eagle Ford sections. Sparse unidentified fossil fragments were present throughout all portions of the core. The contact between the Stuart City Limestone and the lower section of the Eagle Ford was noted to be marly and uncharacteristic of the lower portion.

3.2 Geochemical analysis

3.2.1. General X-Ray Fluorescence Results

3.2.1.1 Clay Enrichment

Aluminum (%Al) is cross plotted against major element percentage content to determine a relationship, if any, to the clay content of the core (Figure 3.1).

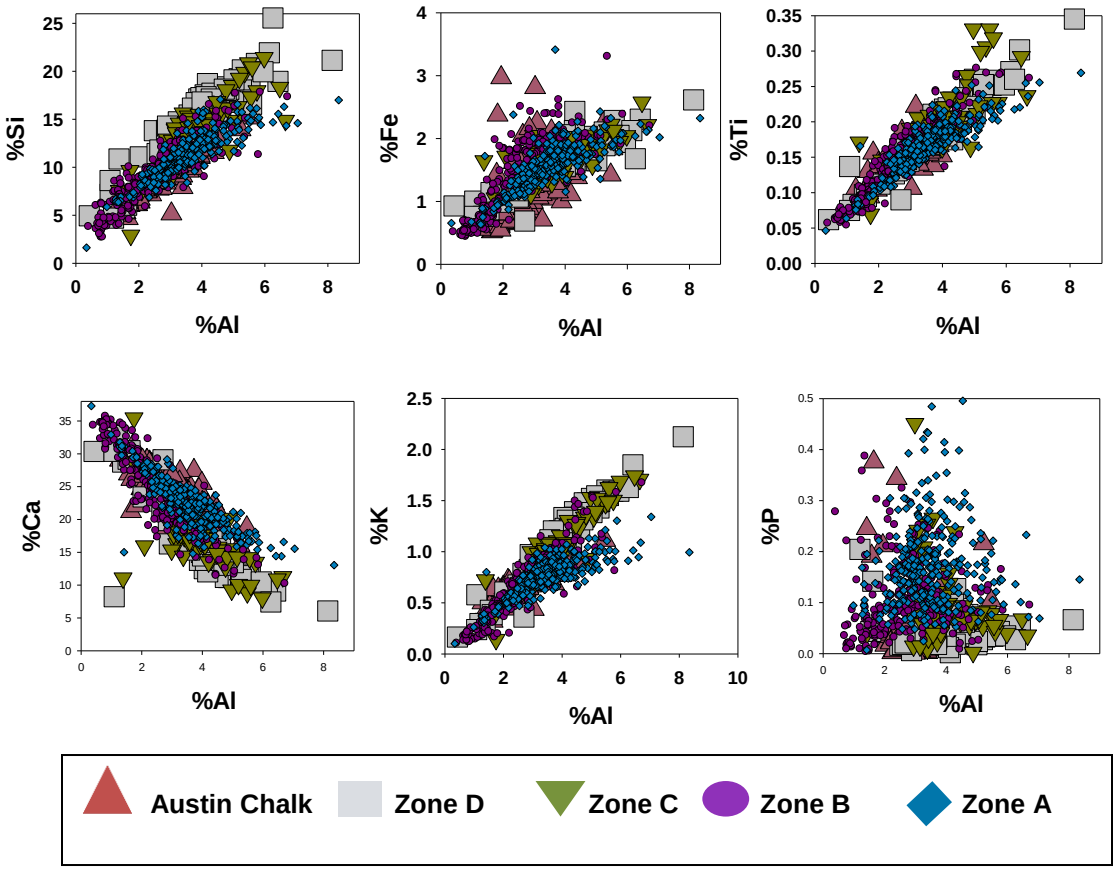

Figure 3.1 Clay Enrichment

Silicon, calcium, potassium, phosphorus, titanium and iron are all shown relative to aluminum (Figure 3.1). Aluminum is used as a proxy for the clay content of the core. Linear trends will indicate a relationship of the element to aluminum and non-linear trends indicate less of (or no) relationship. Silicon, potassium and titanium show linear trends. The trends indicate Si, K and Ti are associated with a clay mineral phase. The deviations in Zones A and B, above the linear trend in silicon, indicate enrichment of silica in possible detrital or biogenic quartz form. The deviations above the trend in titanium indicate titanium is possibly present in another mineral form, potentially rutile (TiO_2). The deviations above the trend in potassium indicate the presence of another mineral phase, possibly K-feldspar ($KAlSi_3O_8$). The phosphorus shows no trend indicating no relationship to the clay fraction of the sediments. The negative slope of the calcium relative to the aluminum indicates the clay content was diluted by calcium deposition.

.

3.2.1.2 Carbonate phases

As stated before, the calcium shows an inverse trend compared with the aluminum (Figure 3.1). There is also a negative component to the sulfur component. Carbonate dilution of the aluminum and sulfur is likely indicating different depositional situations. Magnesium shows a sub-linear trend with calcium indicating the possibility of a carbonate mineral such as ankerite ($Ca(Fe,Mg,Mn)(CO_2)_3$, or dolomite ($CaMg(CO_3)_2$. Calcium association with phosphates such as francolite $(Ca,Mg,Sr,Na)_{10}(PO_4,SO_8,CO_2)F_{2\text{-}3}$ is also a possibility. Cross plotting the components of phosphates will indicate if relationships exist. The iron, phosphorus and manganese show little to no relationship to the calcium. This indicates the lack of mineral associations between the elements (Figure 3.2).

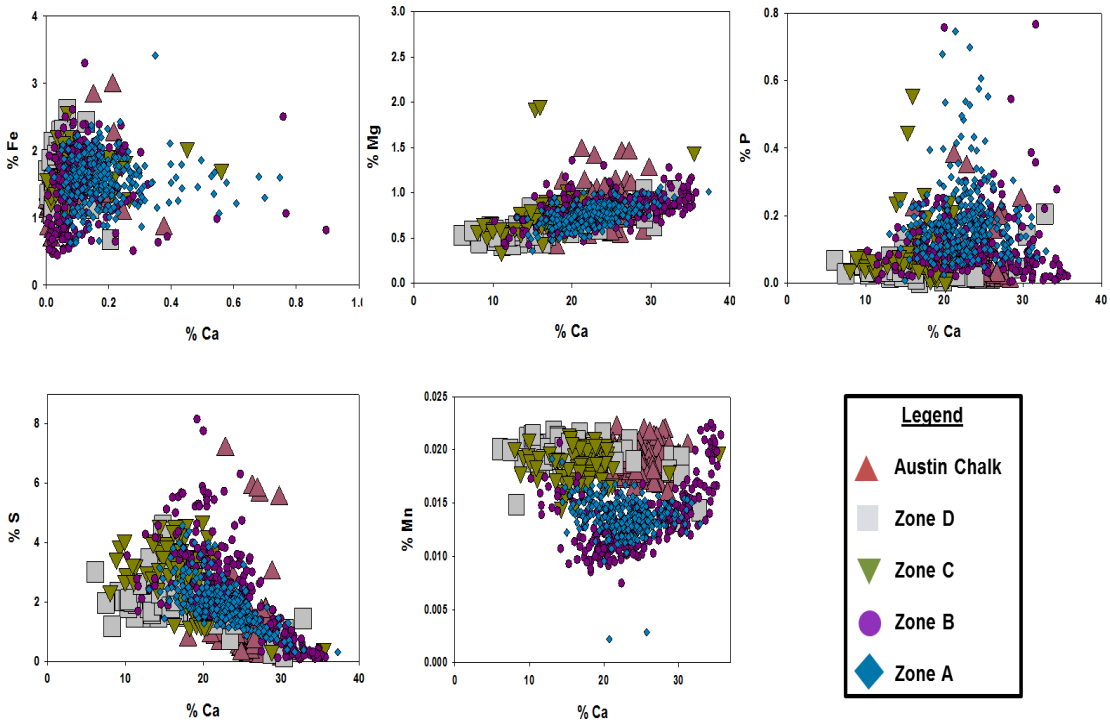

Figure 3.2 Carbonate phases.

3.2.1.3 Calcite-Clay-Quartz Ternary Diagram

When plotted on the calcite-clay-quartz ternary diagram (Figure 3.3), data are strongly aligned along the calcite dilution line, with the majority of the samples trending toward the calcite endmember (Brumsack, 1989). Zone D has more quartz and clay components compared to Zones A and B. This is an indication that the depositional history of the two members is somewhat different. Conditions for calcite formation were more prevalent in the lower section. Aluminum and silicon components increased as the deposit became associated with Zones B and C.

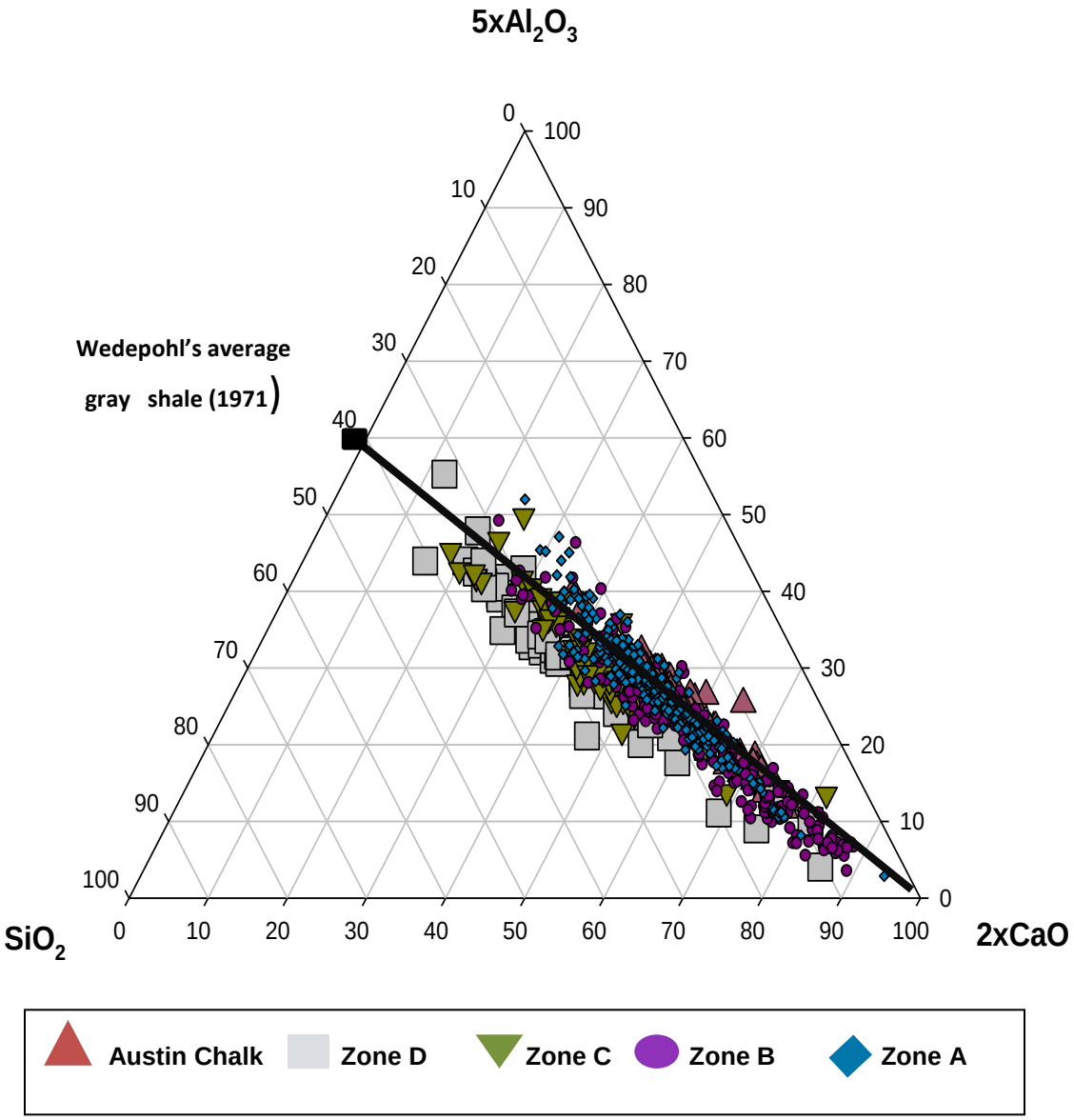

Figure 3.3 Calcite-Clay-Quartz ternary diagram.

3.2.1.4 Pyrite

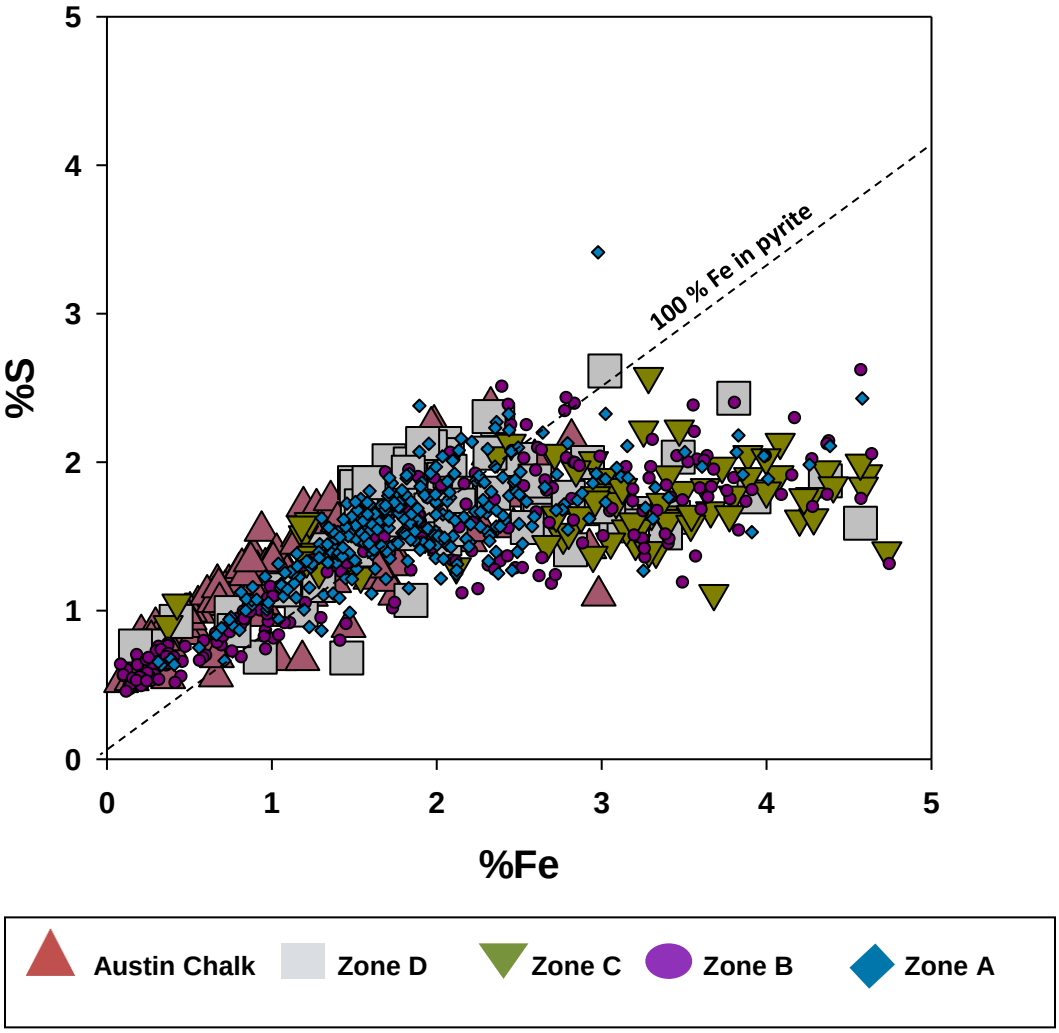

Figure 3.4 Pyrite line. Modified from Raiswell and Berner, 1985.

Sulfur and iron show a strong relationship in Zones A and B (Figure 3.4) and in the Austin Chalk. This is indicative of a pyrite (FeS_2) association. Zone C also shows a lack of relationship to the pyrite content of this core.

3.2.1.5 Major Element Trends

In down core plots (Figure 3.5), the major elements, calcium, iron, phosphorus, aluminum and silicon indicate a pronounced oscillatory pattern in Zones B, C and D indicating the vacillating nature of the depositional mechanisms. For instance, in some zones where calcium has a higher total percentage, silicon, iron and sulfur percentages show a contrasting decrease. The conditions for the calcium deposition are inconsistent with the conditions coeval between the silicon, iron and sulfur in those instances.

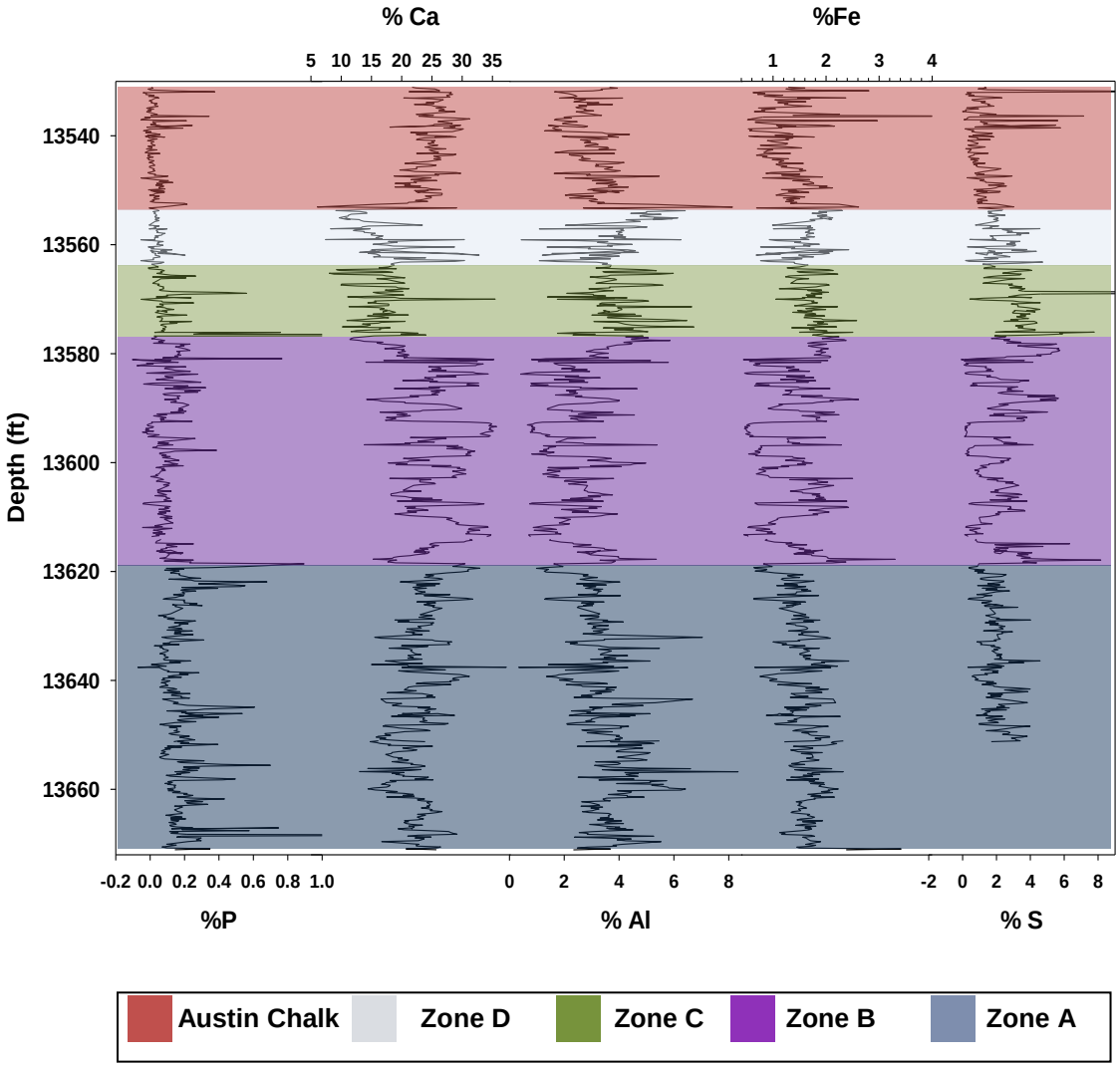

Figure 3.5 Major element trends-XRF

3.2.1.6 Enrichment Factors

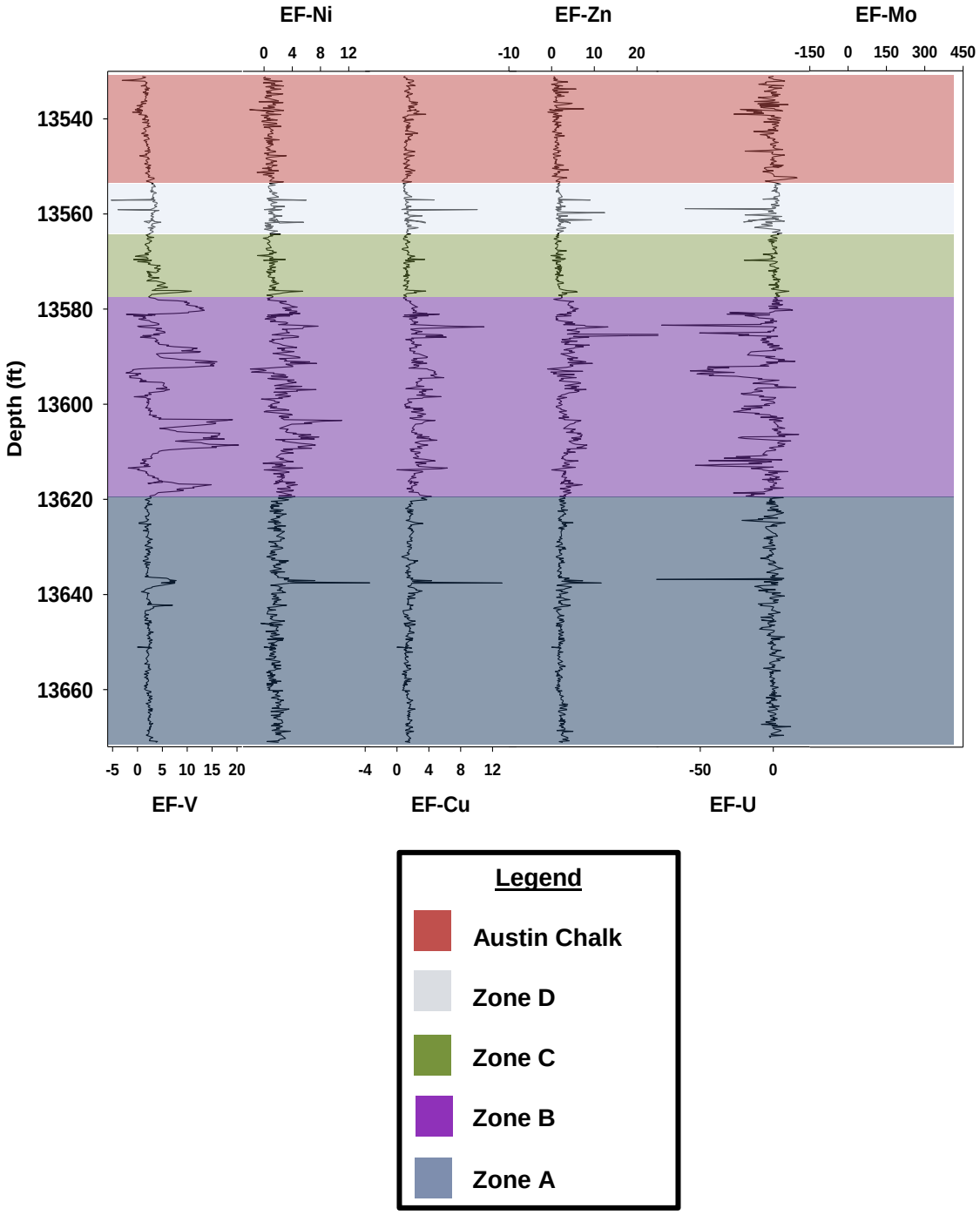

Figure 3.6 Trace element enrichment factors-XRF

When plotting the enrichment factors (EFs) of the trace metal content down core (Figure 3.6), Zone B indicated significant oscillatory accumulation and depletions. Molybdenum, compared to the average gray shale, is enriched by at least a factor of 300 in some areas of Zone B. Zone D and Zone A also each contains a few enrichment intervals of Mo. In Zone B, vanadium is enriched by a factor of 20 times the amounts attributed to the average gray shale and is oscillatory in nature.

3.2.2 Non XRF Data

3.2.2.1 %TOC, $\delta^{15}N$, $\delta^{13}C$, %N

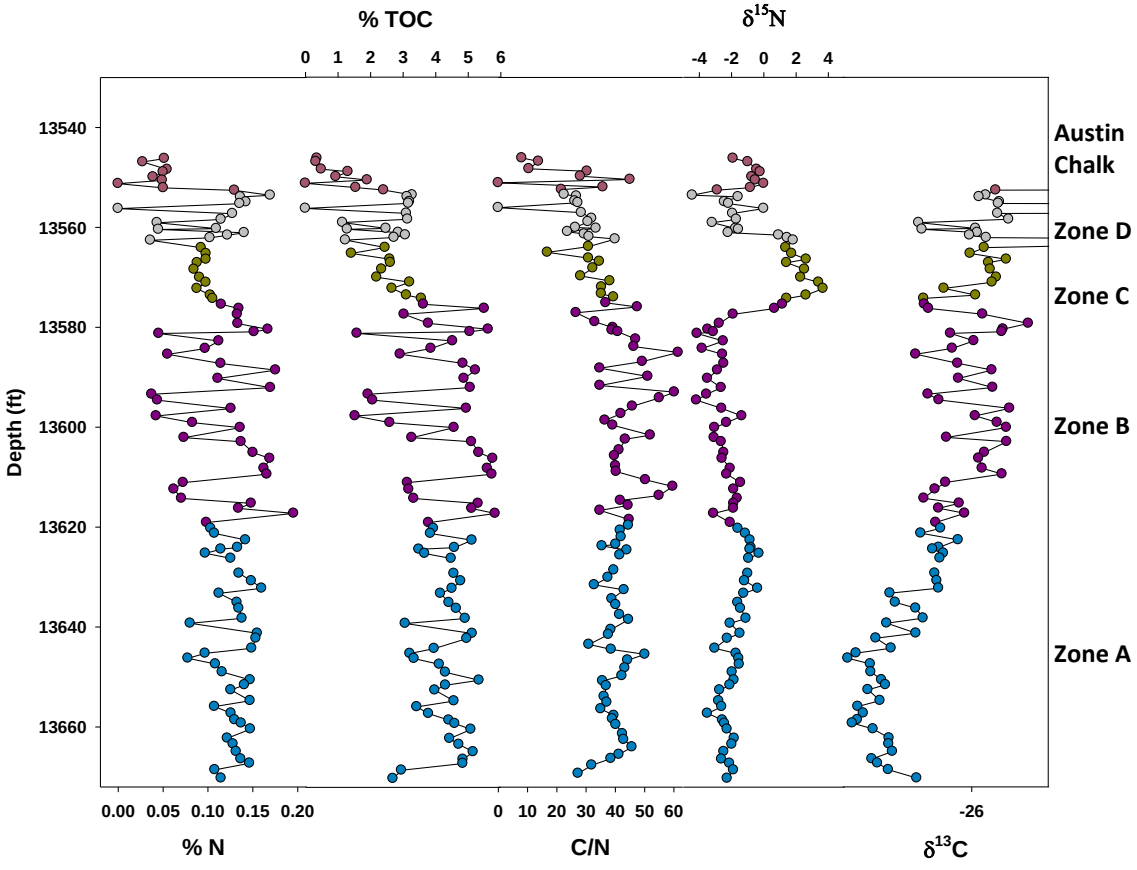

Figure 3.7 Non-XRF data

Isotopic compositions nitrogen and carbon and the total organic carbon (TOC) content were shown to have similar oscillatory patterns in Zone B (Figure 3.7). Fluctuating patterns were illustrated in the above sections when discussing the trace metal content and major element constituents. A relatively pronounced positive excursion of $\delta^{15}N$ in Zones C and D corresponds to a decrease in TOC at that same depth level.

3.2.2.2 XRD Results

In recent data sets, the J.A. Leppard #1 core was found to contain quartz (SiO_2), calcite ($CaCO_3$), gypsum ($CaSO_4$-2(H2O)), pyrite(FeS_2), apatite ($Ca(PO_4)_3(F,Cl,OH)$, illite ($KAl_2(SiO_3AlO_{10})(OH)_2$, kaolinite ($Al_2Si_2O_5(OH)_4$), smectite ($Na,Ca_{).33}(Al, Mg)_2(Si_4O_{10})(OH)_2$-$nH_2O$) and chlorite $(Mg,Fe)_3(Si,Al)_4O_{10}(OH)_2$-$(Mg,Fe)_3(OH)_6$) in variable amounts (Kearns, 2011; Harbor, 2011).

CHAPTER 4

DISCUSSION

4.1 Bulk Geochemistry

4.1.1 Major Elements

Used as a proxy for clay minerals, aluminum was plotted against potassium, iron, silicon and titanium (Figure 3.1). Linear relationships suggest the K, Si and Ti are all largely associated with the clay components. However, the positive enrichment trends of the Zone C and D samples suggest, these elements are present in additional phases. Iron shows a slight linearity with aluminum. This suggests that a small portion of Fe is bound in clay and a large portion of the Fe is in another phase, e.g. pyrite. The presence of pyrite (FeS_2) was confirmed in hand samples, cross plots of sulfur and iron (Figure 4.2), and in XRD analysis. The samples showed two different relationships between sulfur and iron. A portion of the core has pyrite deposition and the other portion has Fe and S present in other phases.

Calcium showed a slight association with magnesium. This is indicative of calcium-magnesium mineral phase, perhaps ankerite($Ca(Fe,Mg,Mn)(CO_3)_2$) or dolomite ($CaMg(CO_3)_2$). The negative slope illustrated in the Ca and Al cross plot demonstrates that a significant portion of calcium diluting the aluminum phases in this core. Calcium and sulfur also show a dilution trend suggesting the amount of calcium is obscuring the minor mineral phases of gypsum ($CaSO_4$-$2(H_2O)$) found in XRD data.

The Austin Chalk and the Eagle Ford plot in the mid-range of shale on the calcite-clay-quartz ternary diagram (Figure 3.3). Zones C and D include silica/aluminum and calcium end members suggestive of dilution effects at both ends of the spectrum present in the same section.

4.1.2 Trace Elements and TOC

Trends with total organic content (%TOC) and the trace metals copper (Cu), zinc (Zn) and nickel (Ni) suggest a moderate association. These trace metals have been associated with environmental micronutrients and primary production (Figure 4.1)

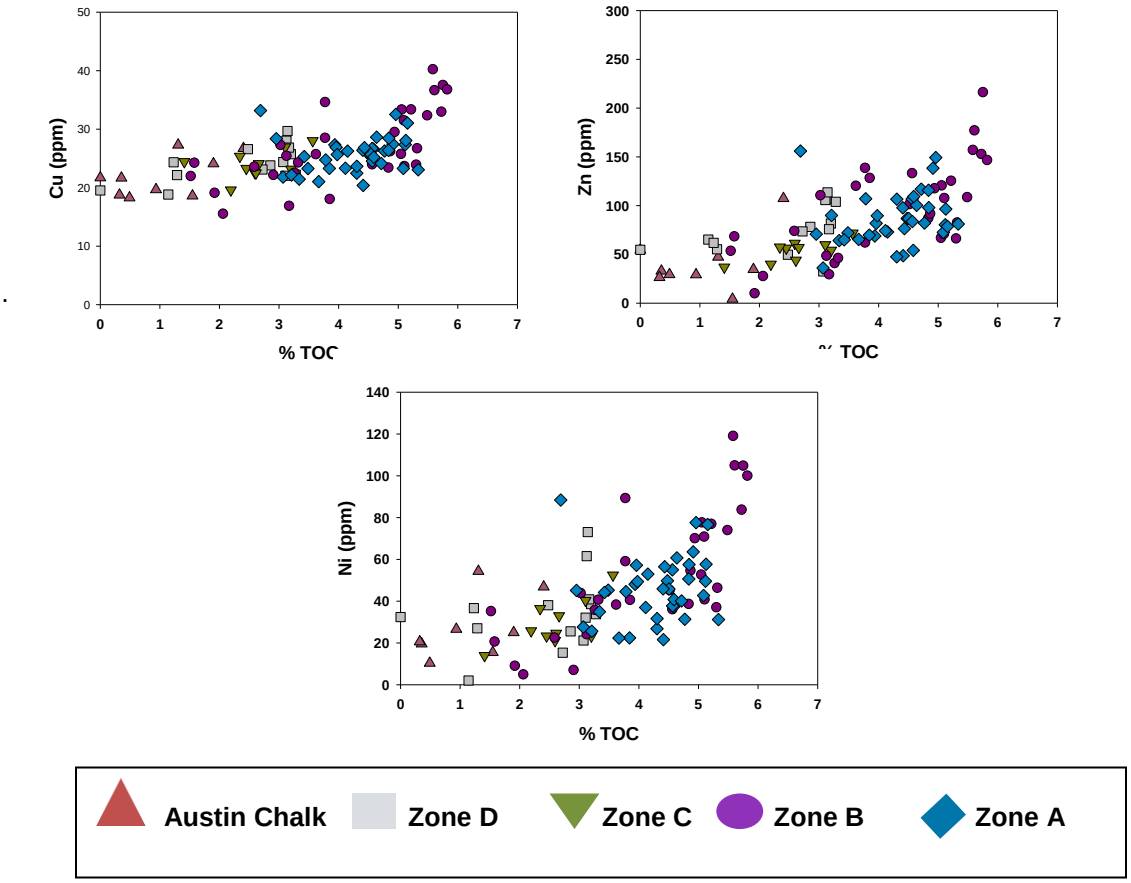

Figure 4.1 Productivity proxies

The %TOC content is used as a paleo-proxy for primary productivity. The large variances of %TOC values (Figure 3.7) in Zone B, from 0% to more than 6% are indicating productivity was prolific at times and extremely depleted in others.

4.1.3 Degree of Pyritization

The degree of pyritization (DOP_T) is often used as a proxy to evaluate bottom water redox conditions. DOP_T values less than 0.42 are considered oxic, values in the range between 0.46 and 0.80 are indicative of dysoxic conditions and for combined anoxic/euxinic conditions, DOP_T levels are considered to lie between 0.55 and 0.93 (Raiswell and Berner, 1986). With levels falling below .42 in Zone C (Figure 4.2), there is an indication of an oxic water column during some intervals in the Eagle Ford. However, most of the samples are in the range of the anoxic/euxinic levels.

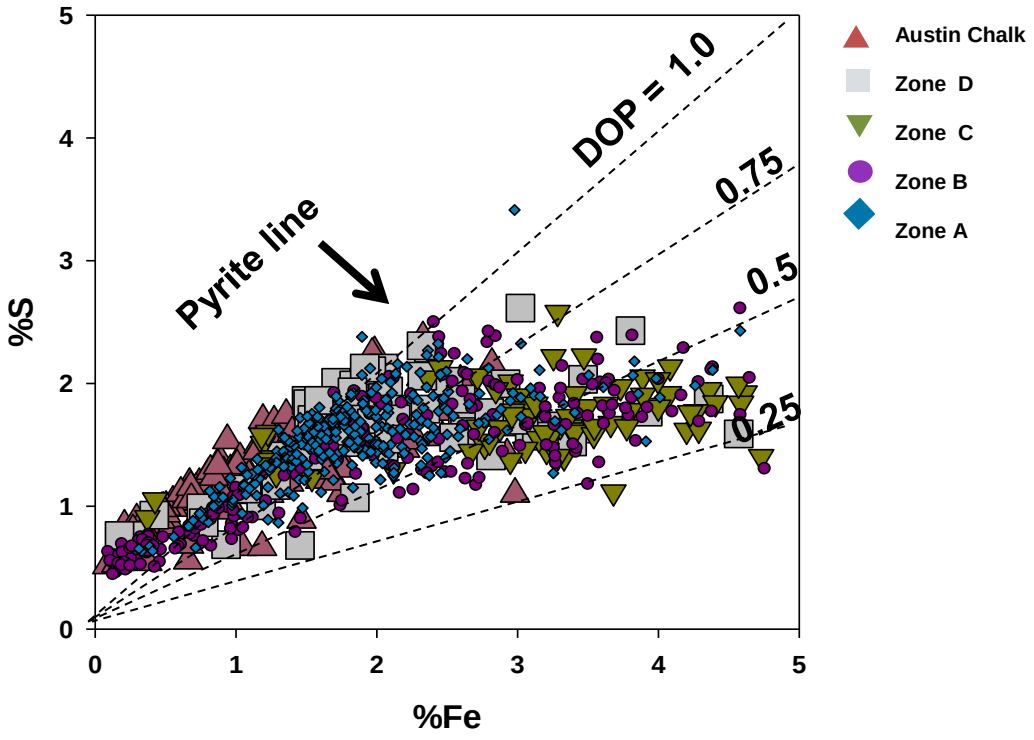

Figure 4.2 Degree of pyritization

4.2 Paleoceanography

4.2.1 Redox Indices

Enrichment factor values (EFs) near 1 indicate similarity to an average shale abundance of that element and normal marine, or oxic conditions. Increase in values above this number indicate deposition under anoxic or euxinic marine conditions. The cyclical natures of the EFs of Zone B in the Eagle Ford suggest rapid shifts in marine conditions (Figure 3.6). The positive EFs of molybdenum, zinc, copper, nickel, and vanadium are mostly coincident with each other through Zone B. EFs indicating conditions similar to normal marine waters occurred with the same comparable cyclicity. There are six different pronounced cycles of oxic to anoxic/euxinic water column conditions in Zone B.

A comparison of the DOP_T, %TOC and EFs (molybdenum and iron) has been plotted to indicate the level of oxygenation in the water column (Figure 4.3). This chart corroborates with the EF indicators that there were mostly anoxic/euxinic conditions throughout most of the Eagle Ford deposition. A small percentage of samples lie in the oxic zone indicating normal marine conditions were intermittently present.

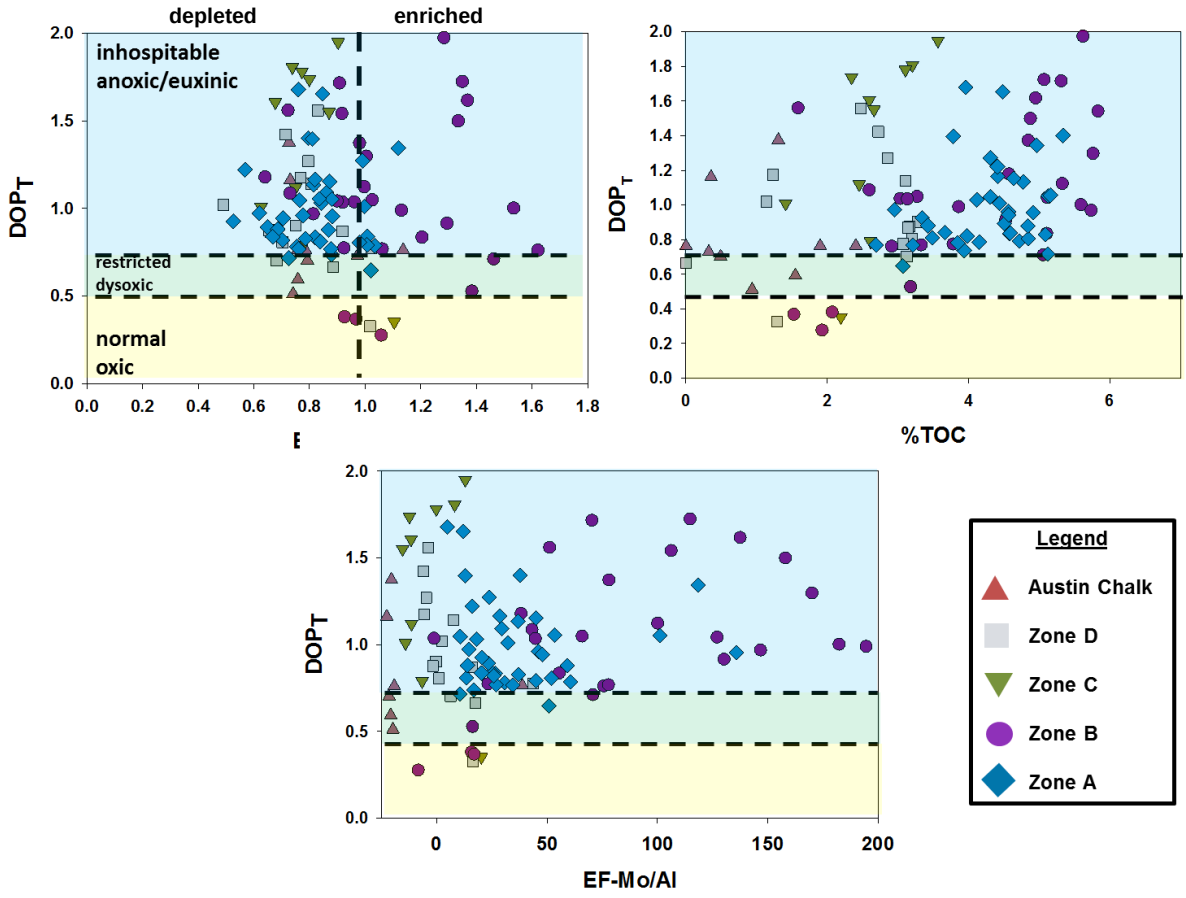

Figure 4.3 Oxic, dysoxic and inhospitable conditions. Modified from Rowe et al., 2008

4.2.2 Paleoproductivity

Stable isotope ratios of nitrogen can also be indicative of nitrogen cycling related to enhanced productivity and suboxic conditions in the water column (Meyers 1997; Twichell et al., 2002; Meyers et al., 2009A). From Zone A of the lower Eagle Ford, the $\delta^{15}N$ shows a relatively stable curve throughout most of the core until a distinct negative excursion is pronounced at the beginning of Zone B (Figure 3.7). At Zone C, the $\delta^{15}N$ exhibits a dramatic positive excursion. The drop in the $\delta^{15}N$ is perhaps an indicator of enhanced productivity and the positive excursion could mark a drop in that activity.

Enhanced C/N ratios are also indicative of increased productivity. The J.A. Leppard core has dramatic shifts in the ratio with an overall negative shift at the beginning of Zone C. This is possibly related to the drop in productivity.

The positive shift in $\delta^{13}C$ at Zone D could be due to increased carbonate production. Coupled with the Sr/Ca ratio (Figure 4.4) that also shows a positive shift during the deposition of Zone D, calcareous nannofossil production could have had an increase in response to changing water column conditions (Stoll and Schrag, 2001).

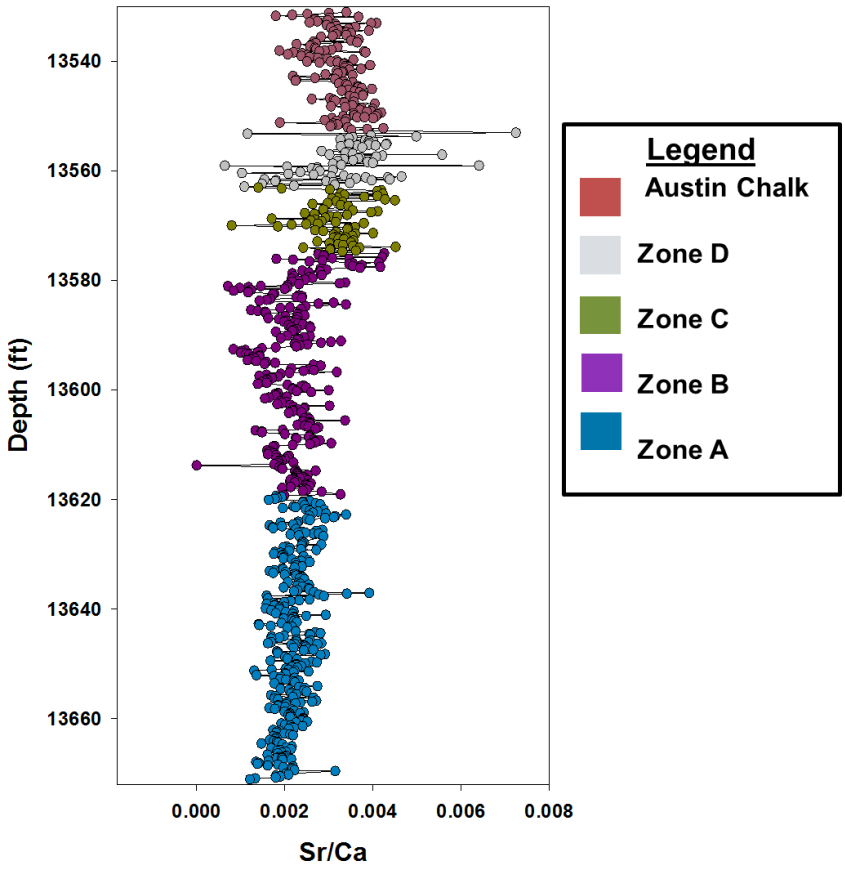

Figure 4.4 Strontium/Calcium ratio versus depth.

. 4.2.3 Physical Paleoceanography

The %TOC and molybdenum (ppm) were also used to indicate increased basinal restriction and deep-water age of the deposits (Figure 4.5). Zone A in the lower Eagle Ford and Zone C show two different depositional regimes. A majority of the samples plotted within an extremely restricted basin. The other portion of the samples plotted in a more open environment. This is likely due to an increase of transgressive flooding events during the deposition of the Eagle Ford Formation changing the water column from anoxic/euxinic conditions to a more oxic normal marine setting.

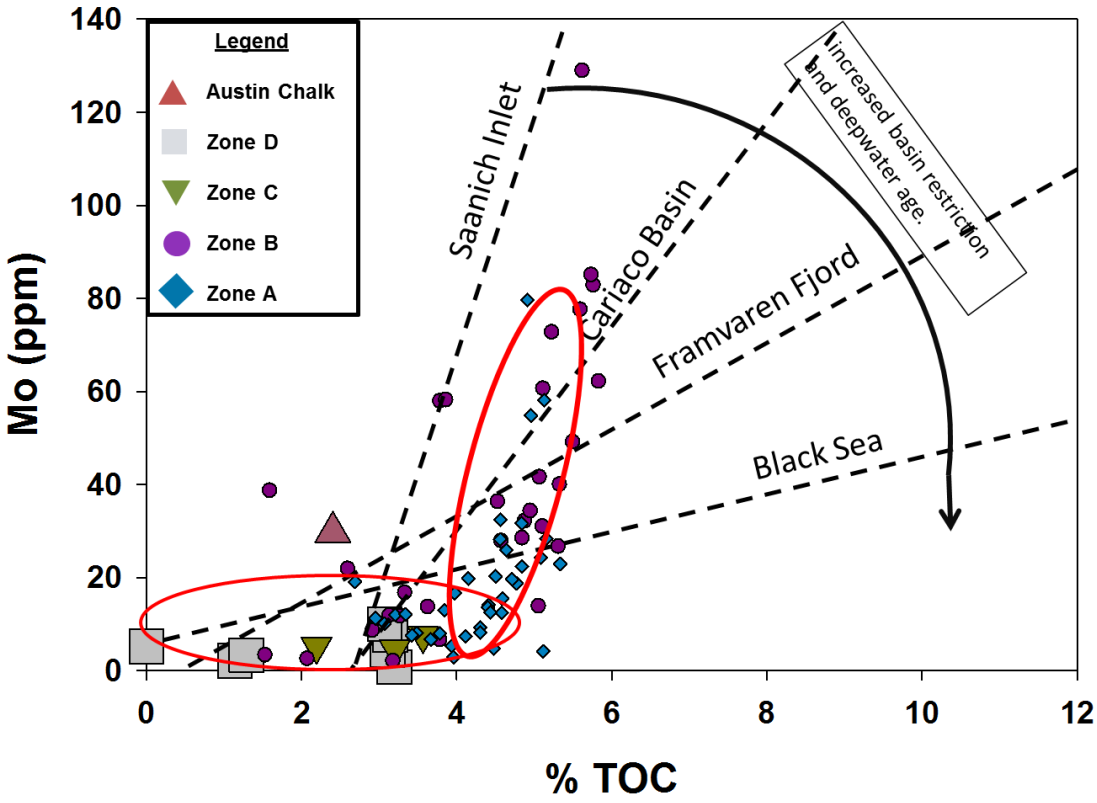

Figure 4.5 Basin restriction and deepwater age. Modified after Algeo and Rowe, 2012

CHAPTER 5

CONCLUSIONS

By utilizing geochemical proxies, the Eagle Ford Formation was shown to have been deposited both in an oxic, sub-oxic and anoxic/euxinic environment. With partially restricted basin hydrography apparent in some portions of the core, some open marine conditions, and other portions of the core exhibiting a more restricted environment, the Eagle Ford showed multiple depositional environments. Mineralogical data confirmed the calcareous nature of the sediment with small detrital influences.

Trace metal accumulation was enriched where the marine conditions were dysoxic and/or anoxic/euxinic. The total organic content of the core was high in the areas associated with basin restriction and inhospitable conditions.

Geochemical analysis of the J.A. Leppard #1 core revealed chemical patterns of cyclicity that were not readily apparent in hand samples or outcrop studies. Five major transgressive events have been chronicled in the Western Interior Seaway of the Cretaceous North America. One of them related to a previously conjectured Cenomanian-Turonian (CT) boundary at the Austin Chalk-Eagle Ford contact. However, biostratigraphic data refutes that particular timing of this event (personal communication, Harry Rowe, 2012).

Biostratigraphic data indicate the positive carbon isotope excursion was recorded in the middle and upper Cenomanian, and the Austin Chalk-Eagle Ford contact was a major unconformity. The Austin Chalk was deposited much later, during the Campanian, not the Turonian.

Instead of relating to the CT boundary and OAE2, the cycling between oxic, normal marine conditions and inhospitable conditions leading up to the positive carbon excursion could be related to another documented OAE, the mid-Cenomainan event (MCE) or the oscillating conditions could also be strictly regional. The cyclical nature of the marine conditions between oxic and inhospitable before global anoxic events could be considered as the preconditioning events leading into OAEs. Understanding the geochemical patterns leading up to major transgressive events and global oceanic perturbations, specifically OAEs, will help to further explain the mechanisms and causal factors involved in such an event.

APPENDIX A

TABLES

Table 2.1. Limits of determination (Rowe, et al., 2012)

Element	Accepted Value[a]	Instrument 1 (UTA-1)			Instrument 2 (1st UTA-2)		
		Measured Value[b]	σ (n=7)[b]	LDM[c]	Measured Value[b]	σ (n=7)[b]	LDM[c]
Mg (%)	0.67	0.80	0.09	0.17	0.85	0.14	0.28
Al (%)	4.96	5.39	0.14	0.28	5.32	0.11	0.22
Si (%)	32.6	33.7	0.2	0.5	33.1	0.4	0.8
P (%)	0.07	0.05	0.03	0.07	0.09	0.03	0.06
S (%)	3.34	2.18	0.10	0.20	2.27	0.09	0.18
K (%)	2.07	2.31	0.09	0.18	2.22	0.07	0.14
Ca (%)	0.13	0.23	0.03	0.06	0.24	0.02	0.04
Ti (%)	0.23	0.27	0.02	0.04	0.27	0.02	0.03
Mn (%)	0.015	0.012	0.001	0.002	0.013	0.001	0.003
Fe (%)	2.93	2.55	0.06	0.12	2.52	0.06	0.13
Ba (ppm)	2090	1884	376	753	1706	300	600
V (ppm)	928	1114	68	137	1110	80	159
Cr (ppm)	110	98	13	26	106	14	27
Ni (ppm)	130	153	26	52	150	20	40
Cu (ppm)	83	147	20	40	87	12	23
Zn (ppm)	823	844	96	191	880	74	147
Th (ppm)	8.4	9	1	2	9	1	2
Rb (ppm)	122	123	12	25	131	12	25
U (ppm)	18.1	17	6	11	22	4	8
Sr (ppm)	75.5	87	5	10	93	9	18
Y (ppm)	35.4	34	3	5	36	2	4
Zr (ppm)	80.3	95	7	13	96	6	13
Nb (ppm)	9	9	1	2	9	1	2
Mo (ppm)	79	83	4	9	82	3	6

a Values for major elements from lithium borate-fused disc analysis by WD-XRF at SGS; values for trace elements (ppm) from sodium borate fusion dissolution and analysis by ICP-MS
b Average HH-ED-XRF measured values (n = 7) and standard deviations for reference material RTC-W-260, a black shale from the Devonian Woodford Formation of West Texas.
c Limit of Determination of a Method (LDM) calculated according to Rousseau (2001

REFERENCES

Algeo, T.J., Maynard, J.B., 2004, Trace-element behavior and redox facies in core shales of Upper Pennsylvanian Kansas-type cyclothems, Chemical Geology, v. 206, is. 3-4, p. 289-318.

Algeo, T.J., Lyons, T.W., Mo-total organic carbon covariation in modern anoxic marine environments: implications for analysis of paleoredox and paleohydrographic conditions, Paleooceanography, v. 21, p. 1-23.

Algeo, T.J., Heckel, J.B., Maynard, Blakey, R., Rowe, H., 2008, Modern and ancient epicratonic seas and superestaurine circulation model of marine anoxia, in Holmden and BR Prat, (Eds). Dynamics of Epeiric Seas, Paleontological and Geochemical Perspectives: Geological Association of Canada Special Publication, Vol. 48, p. 7-38.

Algeo, T.J., Tribovillard, N., 2009, Environmental analysis of paleoceanographic systems based on molybdenum-uranium covariation, Chemical Geology, v. 268, p. 211-225.

Algeo, T.J., Rowe, H., 2012, Paleoceanographic applications of trace-metal concentration data, Chemical Geology, v. 324-325, p. 6-18.

Arthur, M.A., Dean, W.E., Pratt, L.M., 1988, Geochemical and climatic effects of increased marine organic carbon burial at the Cenomanian/Turonian boundary: Nature, v. 335, p. 714-717.

Arthur, M.A. and Sageman, B.B., 1994, Marine Black Shales: Depositional Mechanisms and Environments of Ancient Deposits: Annual Reviews of Earth Planetary Science, v. 22, p. 499-551.

Arthur, M.A. and Schlanger, S.O., 1979, Cretaceous "Oceanic Anoxic Events" as Causal Factors in Development of Reef-Reservoired Giant Oil Fields, The American Association of Petroleum Geologists Bulletin, v. 63, vo. 6. p. 870-885.

Arthur, M.A., Schlanger, S.O., Jenkyns, H.C. 1987, The Cenomanian-Turonian oceanic anoxia event: II. Paleoceanographic controls on organic matter production and preservation. Geological Society, London, Special Publications, Vol. 26, p. 401-420.

Berner, R.A., and Raiswell, R., 1983, Burial of organic carbon and pyrite sulfur in sediments over Phanerozoic time: a new theory: Geochemica et Cosmochimica Acta, Vol. 47, Issue 5, p. 855-862.

Blakey, R., 1994, Global Paleogeography, Northern Arizona University. <http://www2.nau.edu/rcb7/nam.html>, Accessed November, 2012.

Brown, C.W., and Pierce, R.L., 1962, Palynologic correlations in Cretaceous Eagle Ford Group, northeast Texas: American Association of Petroleum Geologists Bulletin, v. 46, p. 2133-2147.

Brumsack, H.J., 2006, The trace metal content of recent organic carbon righ sediments: Implications for cretaceous black shale formation, Palaeogeography, Palaeoclimatology, Palaeoecology 232, is. 2-4, p. 344-361.

Calvert, S.E., 1987, Oceanographic controls on the accumulation of organic matter in marine sediments. Geological Society, London, Speical Publications, v. 26, 137-151.

Calvert, S.E., Pedersen, T.F., 1993, Geochemistry of recent oxic and anoxic marine sediments: implications for the geological record. Marine Geology.v. 113, p 67-88.

Coccioni, R., Galeotti, S., 2003. The mid-Cenomanian Event: prelude to OAE 2, Palaeogeography, Palaeoclimatology, Palaeoecology, v. 190. p. 427-440.

Comet, P.A., Rafalska, J.K., Brooks, J.M., 1993, Sterane and tritepane patterns as diagnostic tools in the mapping of oils, condensates and source rocks of the Gulf of Mexico region. Organic Geochemistry, vol. 20, Issue 8, p. 1265-1296.

Crusius, J., Calvert, S., Pedersen, T., Sage, D., 1996, Rhenium and molybdenum enrichments in sediments as indicators of oxic, suboxic and sulfidic conditions of deposition. Earth and Planetary Science Letter, v. 145, p. 65-78.

Dawson, W.C., Katz, B.J., Liro, L.M., Robison, V.D., 1993, Stratigraphic and Geochemical Variability: Eagle Ford Group, East-Central Texas, GCSSEPM Foundation 14th Annual Research Conference, Rates of Geologic Process, Dec. 5-8.

Dawson, W.C., 1997, Shale microfacies: Limestone microfacies and sequence stratigraphy: Eagle Ford Group (Cenomanian-Turonian) north-central Texas outcrops. Gulf Coast Association of Geological Societies Transactions, v. 47, p. 99-105.

Dawson, W.C., 2000. Shale microfacies: Eagle Ford Group (Cenomanian-Turonian) north-central Texas outcrops and subsurface equivalents: Gulf Coast Association of Geological Societies Transactions, v. 50, p. 607-621.

Dean, W.E. and Arthur, M.A., 1989. Iron-Sulfur relationships in Organic-Carbon Rich Sequence I: Cretaceous Western Interior Seaway. American Journal of Science, v. 289. p. 708-743.

Donovan, A.D., and Staerker, T.S., 2010, Sequence Stratigraphy of the Eagle Ford (Boquillas) Formation in the Subsurface of South Texas and Outcrops of West Texas: Gulf Coast Association of Geological Societies Transactions, v. 60, p. 861-899.

Gale, A.S., Voight, S., Sageman, B.B., Kennedy, W.J., 2008, Eustatic sea-level record for the Cenomanian (Late Cretaceous)-Extension to the Western Interior Basin, USA, Geology, v. 36, p. 859-862.

Gordon, C.H., 1911, Geology and underground waters of northeastern Texas: U.S. Geological Survey Water Supply Paper 276. 78 p.

Handoh, I.C., Lenton, T.M., 2003, Periodic mid-Cretaceous oceanic anoxic events linked by oscillations of the phosphorus and oxygen biogeochemical cycles, Global Biogeochemical Cycles, v. 17, no. 4, 1092

Haq, B.U., Hardenbol, J., Vail, P.R., 1986, Chronology of fluctuating sea levels since the Triassic (250 million years ago to present), Science, v. 235, p. 1156-1167.

Harbor, R.L., 2011, Facies Characterization and Stratigraphic Architecture of Organic-Rich Mudrocks, Upper Cretaceous Eagle Ford Formation: MS thesis, University of Texas at Austin. 184 p.

Hastings, D.W., Emerson, S.R., Erez, J., Nelson, B.K., 1996, Vanadium in foraminiferal calcite: Evaluation of a method to determine paleo-seawater vanadium concentrations, Geochimica et Cosmochimica Acta, v. 60, is. 19, p. 3701-3715.

Hentz, T.F., and Ruppel, S.C., 2010, Regional lithostratigraphy of the Eagle Ford Shale: Maverick Basin to East Texas Basin: Gulf Coast Association of Geological Societies Transactions, v. 60, p 325-337.

Hentz, T.F., and Ruppel, S.C., 2011, Regional Stratigraphic and Rock Characteristics of Eagle Ford Shale In Its Play Area: Maverick Basin to East Texas Basin. AAPG Annual Convention, Houston, Texas 2011. Search and Discovery Article #10325

Hetzel, A., Bottcher, M.E., Wortmann, U.G., Brumsack, H.J., Paleo-redox conditions during OAE2 reflected in Demerara Rise sediment geochemistry (ODP Leg 2070, Palaeogeography, Palaeoclimatology, Palaeoecology, v. 273, p. 302-328.

Hill, R.T., 1901, Geography and geology of the Black and Grand Prairies, Texas: USGS 21st Annual Report, pt. 7, 666 p.

Jenkyns, H.C., 1980, Cretaceous anoxic events: from continents to oceans, Journal of the Geological Society of London, v. 137. p. 171-188.

Jenkyns, H.C., 2010, Geochemistry of oceanic anoxic events, Geochemistry, Geophysics, Geosystems, v. 11 p. 1-30.

Jiang, Ming-Jung, 1989, Biostratigraphy and geochronology of the Eagle Ford Shale, Austin chalk, and lower Taylor marl in Texas based on calcareous nannofossils. (Volumes I and II), Phd dissertation, Texas A&M University.

Jones, B., Manning, D.A.C., 1994, Comparison of geochemical indices used for the interpretation of palaeoredox conditions in ancient mudstones, Chemical Geology, v. 111, is.1-4, p. 111-129.

Jones, C.E., Jenkyns, H.C. 2001, Seawater strontium isotopes, oceanic anoxic events, and seafloor hydrothermal activity in the Jurassic and Cretaceous, American Journal of Science, v. 301, p. 112-149.

Kauffman, E.G., 1977, Cretaceous facies, faunas and paleoenvironments across the western interior basin: The Mountain Geologist, Field guide: North American Paleontological Convention II, 274 p.

Kauffman, E.G., 1984, Paleobiogeography and Evolutionary Response Dynamic in the Cretaceous Western Interior Seaway of North America. Geological Association of Canada Special Paper, 27

Kearns, T.J., 2011, Chemostratigraphy of the Eagle Ford Formation, MS Thesis, University of Texas at Arlington, 254 p.

Keller, G. and Pardo, A., 2005, Age and paleoenvironment of the Cenomanian-Turonian global stratotype section and point at Pueblo, Colorado: Marine Micropaleontology, v. 51, p. 95-128.

Kolonic, S., Wagner, T., Forester,A., Sinninghe Damste, J.S., Walsworth-Bell, B., Erba, E., Turgeon, S., Brumsack, H.J., Chellai, E.H., Tsikso, H., Kuhnt, W., Kuypers, M.M.M.,2005, Black shale deposition on the northwest African shelf during the Cenomanian/Turonian oceanic anoxic event: Climate coupling and global organi carbon burial. Paleoceanography, v.20.

Kuypers, M.M.M., Blokker, P., Erbacher, J., Kinkel, H., Pancost, R.D., Schouten, S., Sinninghe Damste, J.S., 2001. Massive Expansion of Marine Archaea During a Mid-Cretaceous Oceanic Anoxic Event. Science, v. 293, p. 92-94.

Leckie, R.M., Bralower, T.J., Cashman, R., 2002, Oceanic anoxic events andplankton evolution: Biotic response to tectonic forcing during the mid-Cretaceous, Paleoceanography, v. 17, 29 p.

Liro, L.M., Dawson, W.C., Katz, B.J., Robinson, V.D., 1994, Sequence Stratigraphic Elements and Geochemical Variability within a "Condensed Section": Eagel Ford Group, East-Central Texas. Gulf Coast Association of Geological Societies Transactions. v. 44, p. 393-402.

Lock, B.E., Pechier, L., 2006, Boquillas (Eagle Ford) Upper Slope Sediements, West Texas: Out crop Analogs for Potential Shale Reservoirs, GCAGS Annual Convention, AAPG Search and Discovery article #90056

Lock, B.E., Bases, F.S., and Glaser, R.A., 2007, The Cenomanian sequence stratigraphy of Central to West Texas: Gulf Coast Association of Geological Societies Transactions, v. 57, p. 465-479.

Mancini, E.A., and Puckett, T.M., 2005, Jurassic and Cretaceous transgressive-regressive (T-R) cycles, northern Gulf of Mexico, USA: Stratigraphy, v. 2, p. 31-48.

Mancini, E.A., Puckett, T.M., Tew, B.H., 1996, Integrated biostratigraphic and sequence stratigraphic framework for Upper Cretaceous strata of the eastern Gulf Coastal Plain, USA: Cretaceous Research, v. 17, p. 645-669.

McNulty, C.L., 1966, Nomenclature of upper-most Eagle Ford formation in northeastern Texas; American Association of Petroleum Geologists Bulletin, v. 50, p 375-379.

Meyers, P.A., Dunham, K.W., Ho, E.S., 1988, Organic geochemistry of Cretaceous black shales from the Galicia Margin, Ocean Drilling Program Leg 103, Advances in Organic Geochemistry, v. 13, p. 89-96.

Meyers, P.A., 1994, Preservation of elemental and isotopic source identification of sedimentary organic matter, Chemical Geology, v. 114, p. 289-302.

Murry, G.E., Ata-Ur-Rahman, Yarborough, H., 1985, Introduction to the habitat of petroleum, northern Gulf (of Mexico) Coastal Province, in B.F. Perkins and G.B. Martin, eds., Habitat of oil and gas in the Gulf Coast: Proceedings of the 4th Annual Gulf Coast Section of the Society of Economic Paleontologists and Mineralogists Foundatin Research Conference, Houston, Texas, p. 1-24.

Pessagno, E.A., 1969, Upper Cretaceous stratigraphy of the western Gulf Coast area of Mexico, Texas and Arkansas: Geological Society of America Memoir 111, 139 p.

Phelps, R.M., 2011, Middle-Hauterivian to Lower-Campanian Sequence Stratigraphy and Stable Isotope Geochemisty of the Comanche Platform, South Texas; Phd Dissertation, The University Of Texas, Austin, Texas, 240 p.

Piper, D.Z., 1994, Seawater as the source of minor elements in black shales, phosphorites and other sedimentary rocks, Chemical Geology, v. 114, is. 1-2, p. 95-114.

Piper, D.Z., Perkins, R.B., 2004, A modern vs. Permian black shale-the hydrography, primary productivity, and water-column chemistry of deposition, Chemical Geology, v. 206, is. 3-4, p. 177-197.

Railroad Commission of Texas, 2012, Eagle Ford Information, <http://www.rrc.state.tx.us/eagleford/index.php#general>, accessed November 2012.

Rimmer, S.M., 2004. Geochemical paleoredox indicators in Devonian-Mississippian black shales, Central Appalachian Basin (USA), Chemical Geology v. 206, p. 373-391.

Rousseau, R.M., 2001, Detection limit and estimate of uncertainty of analytical XRF results: The Rigaku Journal, v. 18, p. 33-47.

Rowe, H.D. and Hughes, N., 2010, Strategy for Developing and Calibrating Shale and Mudstone Chemostratigraphies Using Hand-Held X-Ray Fluorescence Units, AAPG Annual Convention, Unmasking the Potential of Exploration and Production. Search and Discovery Article #90104.

Rowe, H., Hughes, N., Robinson, K., 2012. The quantification and application of handheld energy-dispersive x-ray fluorescence (ED-XRF) in mudrock chemostratigraphy and geochemistry, Chemical Geology, 324-325, 122-131.

Rowe, H.D., Loucks, R.G., Ruppel, S., Rimmer, S.M., 2008, Mississippian Barnett Formation, Fort Worth Basin, Texas: Bulk geochemical inferences and Mo-TOC constraints on the severity of hydrographic restriction: Chemical Geology v. 257, p. 16-25.

Schlanger, S.O. and Jenkyns, H.C., 1976, Cretaceous oceanic anoxic events: causes and consequences, Geologie en Mijnbouw, v. 55. p. 179-184.

Scott, R.W., 2010, Cretaceous Stratigraphy, Depositional Systems, and Reservoir Facies of the Northern Gulf of Mexico. Gulf Coast Association of Geological Societies Transactions, v. 60, p. 597-609.

Sellards, E.H., Adkins,W.S., Plummer, F.B., 1932, The geology of Texas,I: Stratigraphy: The University of Texas Bulletin No. 3232, p 422-439.

Sohl, N.F., and Smith, C.C., 1980, Notes on Cretaceous biostratigraphy: American Geological Institute, Excursions in Southeastern Geology, v. 2, Alexandria, Virginia, p. 392-402.

Stoll, H.M., Schrag, D.P., 2001, Sr/Ca variations in Cretaceous carbonates: relation to productivity and sea level changes, Palaeogeography, Palaeoclimatology, Palaeoecology, v. 168, p. 311-336.

Surles, M.A., Jr., 1987, Stratigraphy of the Eagle Ford Group (Upper Cretaceous) and its source-rock potential in the East Texas Basin: Baylor Geological Studies Bulletin, v.45, 57 p.

Twichell, S.C., Meyers, P.A., Diester-Haass, L., 2002, Significance of high C/N ratios in organic-carbon-rich Neogene sediments under the Benguela Current upwelling system, Organic Geochemistry, v. 33, p. 715-722.

Udden, J.A., 1907, A sketch of the geology of the Chisos country, Brewster County, Texas: University of Texas Bulletin 93, Austin, p. 29-33.

Verado, D.J., Froelich, P.N. McIntyre, A., 1990. Determination of organic carbon and nitrogen in marine sediments using the Carlo Erba NA-1500. Deep-Sea Research. v. 37, p. 157-165.

Wedepohl, K.H., 1971, Environmental influences on the chemical composition of shales and clays. In: Ahrens, L.H. Press, F., Runcorn, S.K., Urey, H.C. Eds., Physics and Chemistry of the Earth Pergamon, Oxford, UK, p. 307-331.

BIOGRAPHICAL INFORMATION

Lisa Michelle Moran is a non-traditional returning student. After raising her child and working in service industry laborious jobs, she decided graduate school would provide better opportunities for her family and their success.